



**HAL**  
open science

# Lateritic landsurface-regolith differentiation on Pan-African granitic basement of Adamaoua highland, Cameroon

Mathieu Nouazi Momo, Anicet Beauvais, Romaric Ntchantcho, Paul Tematio

► **To cite this version:**

Mathieu Nouazi Momo, Anicet Beauvais, Romaric Ntchantcho, Paul Tematio. Lateritic landsurface-regolith differentiation on Pan-African granitic basement of Adamaoua highland, Cameroon. CATENA, 2024, 242, pp.108103. 10.1016/j.catena.2024.108103 . hal-04580879

**HAL Id: hal-04580879**

**<https://hal.science/hal-04580879v1>**

Submitted on 21 May 2024

**HAL** is a multi-disciplinary open access archive for the deposit and dissemination of scientific research documents, whether they are published or not. The documents may come from teaching and research institutions in France or abroad, or from public or private research centers.

L'archive ouverte pluridisciplinaire **HAL**, est destinée au dépôt et à la diffusion de documents scientifiques de niveau recherche, publiés ou non, émanant des établissements d'enseignement et de recherche français ou étrangers, des laboratoires publics ou privés.

1 **Lateritic landsurface-regolith differentiation on Pan-African granitic basement of**  
2 **Adamaoua highland, Cameroon**

3  
4 Mathieu Nouazi Momo<sup>a\*</sup>, Anicet Beauvais<sup>b</sup>, Romaric Ntchantcho<sup>a</sup>, Paul Tematio<sup>c</sup>

5  
6 *<sup>a</sup>Institute of Geological and Mining Research (IRGM), P.O. Box 4110, Yaoundé,*  
7 *Cameroon*

8 *<sup>b</sup>Aix-Marseille Univ, CNRS, IRD, INRAE, CEREGE, BP 80, 13545, Aix-en Provence,*  
9 *Cedex 4, France*

10 *<sup>c</sup>University of Dschang, Faculty of Science, Department of Earth Sciences, P.O., Box*  
11 *67, Dschang, Cameroon*

12  
13  
14  
15  
16  
17  
18  
19 \*Corresponding author: nouazimat@yahoo.fr

20

21 **Abstract** – The aim of this paper is to describe and discuss the laterization pattern and  
22 the structuration mode of land-surfaces formed over the Pan-African granitic basement  
23 of Adamaoua highland. Paleocene to mid-Eocene epeirogeny compartmentalized the  
24 regional topography of Adamaoua on which lateritic landsurfaces have been formed over  
25 granitoids of comparable geochemistry. Regional scale geomorphological observations  
26 and petro-geochemical characterization of lateritic duricrusted regolith allow to  
27 distinguish three distinct lateritic landsurfaces, which are compared to lateritic surfaces  
28 from West Africa. Regolith of the upper and middle landsurfaces incorporate composite  
29 lateritic duricrusts including old bauxites and ferricretes, which are petrological heritages  
30 from former regolith of etch-plain type Paleogene African Surface. On Pan-African  
31 granitic basement of Adamaoua, the upper and middle landsurfaces formed on granitoids  
32 before mid-Miocene basaltic-andesitic outpourings that locally cover them, while the  
33 lower landsurface also formed on granitic rocks has been mostly shaped over late  
34 Neogene. The geochemical compositions of lateritic duricrusts of upper and middle  
35 landsurfaces are clearly distributed between aluminous, ferruginous and kaolinite poles  
36 that typifies lateritic regolith of the bauxitic and (Fe-rich) intermediate etch-plains  
37 surfaces similarly as lateritic regolith of the Paleogene West-African sequence.  
38 Geochemical compositions of lateritic regolith on lower landsurface are mostly  
39 distributed between silica, kaolinite and iron, suggesting that more or less evolved or  
40 duricrusted horizons have been exposed by differential erosion of this landsurface.  
41 Lateritic regoliths of the three landsurfaces are also typified and differentiated by their  
42 index of laterization (IOL) and fractionation patterns of some trace (Cr, V, Zr, Ti, Nb, Th,  
43 Y, Ta, Ga) and rare earth elements (HREE, Eu/Eu\*, (Gd/Yb)<sub>N</sub>). Though Neogene  
44 volcanic epirogenic uplift effects on landscape cannot be totally excluded, erosion and  
45 down-wasting of Paleogene landscape mostly evolved to a degraded lateritic etch-plain

46 and late formation of a lower pediplain on Pan-African basement of Adamaoua highland  
47 under long-lasting per-humid climatic conditions over Cenozoic.

48

49 **Keywords:** Lateritic landsurface; Regolith; Trace elements; Rare earth elements;  
50 Adamaoua; Cameroon.

51

## 52 **1. Introduction**

53 Most of lateritic regolith formed across the intertropical belt in landscapes of  
54 cratonic platforms have evolved under relatively quiescent tectonics, depending mostly  
55 from climatic variations over Cenozoic (e.g., Chardon, 2023). Chemical solute  
56 exportations from strongly weathered protoliths resulted in formation of residual Al-Fe  
57 rich lateritic regolith mantling continental scale duricrusted paleosurfaces, e.g., in West  
58 to Central and Eastern Africa (Grandin and Thiry, 1983; Tardy and Roquin, 1998;  
59 Taylor and Howard, 1998; Chardon et al., 2006; Momo Nouazi et al., 2020; Perello et  
60 al., 2020). Most landscapes of the West African intertropical belt consist of numerous  
61 stepped relics of lateritic etching surfaces and pediments above current drainage  
62 networks (e.g., Michel, 1973; Grandin, 1976; Thomas, 1994; Grimaud et al., 2014;  
63 Guillocheau et al., 2015; Chardon et al., 2018; see also Chardon, 2023). The highest  
64 topographies are relics of a continental-scale low-relief erosion paleo-surface (the so-  
65 called African Surface) mantled with thick kaolinitic and bauxitic regolith that have  
66 been produced by intense lateritic weathering during Paleogene (e.g., Beauvais et al.,  
67 2008; Burke and Gunnell, 2008; Beauvais and Chardon, 2013) under greenhouse  
68 climatic conditions (Retallack, 2010; Chardon, 2023). The bauxitic paleosurface,  
69 namely the Paleogene African Surface was then dissected and evolved by successive  
70 erosion and weathering episodes during Oligo-Miocene under tropical contrasted  
71 climates. That resulted in the establishment of an intermediate ferricrete-capped surface  
72 above three stepped lateritic pediments of different ages, which have punctuated  
73 successive denudation stages of the African surface over the Cenozoic (e.g., Beauvais  
74 and Chardon, 2013; Chardon et al., 2018). In the recent decades, dating approaches  
75 using radiometry contributed to better constraining regolith landform dynamics over  
76 geological time scales in West Africa (e.g., Colin et al., 2005; Beauvais et al., 2008), or

77 in Peninsular India (Bonnet et al., 2016; Jean et al., 2020), where similar sequences of  
78 lateritic surfaces have been described and dated.

79 Landscapes of the Adamaoua highland and adjacent plateaus on granitic  
80 Panafrican basement are mostly structured into lateritic etchplains and pediplains  
81 (Martin, 1970). However, geomorphological relics of older lateritic paleosurface (e.g.,  
82 bauxitic or intermediate) are not strictly preserved as well as in West Africa for example  
83 (Michel, 1973; Grandin, 1976; Beauvais and Chardon, 2013; Grimaud et al., 2015;  
84 Chardon et al., 2018). The Adamaoua highland is a swell resulting from a long-  
85 wavelength lithospheric deformation similarly as the one of Central Nigeria (Burke,  
86 2001). Swells owing to early Eocene volcanism (e.g., Fosso et al., 2005; Moundi et al.,  
87 2007) induced regional epirogenic uplift. Resulted landscapes underwent long-term  
88 processes of deep weathering and surface erosion (Segalen, 1967; Michel, 1970; Morin,  
89 1987, 1989; Burke and Gunnell, 2008). Lateritic regolith formed on landsurfaces have  
90 evolved under warm/humid Paleogene to drier Late Neogene changing climatic  
91 conditions (Chardon, 2023).

92 Based on geomorphic, petrologic and geochemical data sets, our objective is to  
93 describe and discuss landscape structuration into three stepped lateritic landsurfaces  
94 upon granitic basement of Adamaoua highland. Compared to West Africa (e.g.,  
95 Beauvais and Chardon, 2013; and Chardon, 2023) geomorphological remnants of old  
96 lateritic surfaces (e.g., bauxitic) are not strictly preserved in current landscapes of  
97 Adamoua. However, numerous petrologic remains of bauxite and ferricrete in surface  
98 regolith betray past wider extension of old lateritic surfaces over crystalline Pan-African  
99 basement of Adamaoua. The importance of these remains allows to typify lateritic  
100 landsurfaces and to reconstitute the landscape evolution on Pan-African Adamaoua.  
101 Considering the available geochronological constraints on volcanic rocks from Eocene

102 (Moundi et al., 1987; Fosso et al., 2005; see also Njonfang et al., 2011), to mid- late  
103 Neogene (Halliday et al., 1988; Marzoli et al. 2000), we also discuss the influence of  
104 resulting epirogeny on topographic changes that potentially maintained persistent  
105 regional paleoclimatic humid regimes, and influenced paleo-landscapes evolution on  
106 Adamaoua highland over Cenozoic. Differences between landscape evolution of  
107 Adamoua highland and West Africa are pointed out and discussed.

108

## 109 **2. Geological and geodynamical framework**

110 The basement of Adamaoua region made up of Neoproterozoic granitoids,  
111 metasedimentary units and migmatites (zircon  $^{207}\text{Pb}/^{206}\text{Pb}$  ages  $\sim 500\text{-}600$  Ma; Toteu et  
112 al., 1987), is part of the northern orogenic belt (mobile zone) of Cameroon (Fig. 1a) that  
113 overthrusts the Archaean Ntem complex (Nzenti et al., 1988). Central Adamaoua  
114 terrains are crossed by the Central Cameroonian Shear Zone, CCSZ, (Fig 1a; Ngako et  
115 al., 2003), which is a trans-lithospheric dextral mobile system of the Pan-African  
116 orogeny (Jorgensen and Bosworth, 1989).

117 The crystalline basement covering  $\sim 70\%$  of Adamaoua is also crossed by the  
118 Cameroon volcanic line (CVL) that instigated a regional epirogenic uplift. Adamaoua  
119 highland is a large horst structure (Deruelle et al., 1991) part of the Central African  
120 component of the swell-and-basin topographic framework (Burke, 2001; Nkouathio et  
121 al., 2008) that also includes the Jos plateau in Nigeria, with the Hoggar, Aïr, Tibesti,  
122 and Darfur highlands (see also Chardon, 2023). The Adamaoua horst has formed and  
123 evolved according to two main stages and is bounded by the Mbere and Djerem grabens  
124 (Deruelle et al., 1991). The first stage corresponds to mid-Cretaceous reactivation of  
125 Precambrian faults, namely distensile NNE-SSW and NW-SE rejuvenations along the  
126  $\text{N}70^\circ\text{E}$  CCSZ (Fig. 1a). This stage led to the extensional opening of South-Adamaoua

127 tectonic grabens and correlative formation of stepped horsts (see also Morin 1989;  
128 Burke, 2001).

129 The second stage corresponds to mantle upwelling between 65 and 30 Ma (Burke,  
130 2001) along thermally thinned and tectonically weakened lithosphere (Fitton, 1980;  
131 Ngako et al., 2006) that resulted in asymmetrical epeirogenic uplift of Adamaoua  
132 basement of ~ 1 km with a southward inclination and fracturing of the horst plateau  
133 along N50-60°E and N130-1400 (Moreau et al., 1987; Nono et al., 1994; Burke, 2001;  
134 Poudjom-Djomani et al., 1997). Mid-Miocene to late Neogene volcanic outpourings  
135 through inherited Precambrian faulting network and fractures (Dautria and Girod, 1986;  
136 Marzoli et al., 2000; Nkouandou et al., 2015) only rejuvenated locally the landscape  
137 topography with emplacement of thick strato-volcanos like Tchabal Nganha of late  
138 Miocene age (Gouthier et al., 1974; Halliday et al., 1988).

139

### 140 **3. Methodological approach**

141 We use field observation stations to describe three stepped landsurfaces between  
142 altitudes 1250 m a.s.l. to  $\leq$  1000 m a.s.l. A field station consists of an area of few square  
143 kilometers, with residual relief(s) preserving relics of at least one specific paleosurface.  
144 At each field station, elevations of relic lateritic surfaces and base levels were recorded  
145 and complemented with petrological characterization of lateritic regolith. Lateritic  
146 duricrusts were described according to the classification by Tardy (1997). Field  
147 observations were complemented by analyzing a combination of digital elevation  
148 models and Google Earth images to extract River long profiles and perform local and  
149 regional synthetic cross sections of lateritic landscapes and 3D interpretation of land  
150 surfaces distribution. Here, we used a Copernicus (COP-30) digital elevation model  
151 (<https://opentopography.org/>) with a spatial resolution of 30 m and a vertical accuracy



152 of <2 m (compared to ~9–12 m of SRTM; Rodriguez et al., 2005) for the Adamawa  
153 region (Airbus, 2020) to extract local relief and topographic metrics.

154 River long profiles have been also extracted to analyze landscape incision pattern,  
155 e.g., location and significance of knick-zones (Figs. 1b-c), and discuss the river  
156 response to climatic and/or litho-tectonic variations (e.g., Grimaud et al., 2014; Marques  
157 et al., 2021). The analysis was undertaken on landforms drained by a major river  
158 network, i.e., the Djerem River drainage system where landscape on Pan-African  
159 basement is composed of three mapped lateritic landsurfaces (Fig. 2a) in central and  
160 southern Adamaoua. Northeastern landscape of Djerem watershed was subject to late  
161 Neogene volcanic activity and outpourings (e.g., see Halliday et al., 1988; Marzoli et  
162 al., 2000) with local topographic uplift.

163 In addition to river long profiles extraction and lateritic landsurfaces mapping, we  
164 described and analyzed petrologic facies of lateritic regolith formed on each landsurface  
165 and their spatial distribution. Major oxides in wt.% and trace + rare earth elements  
166 (REE) in ppm were analyzed by Inductively coupled plasma-atomic emission  
167 spectrometry, ICP-AES, and Inductively coupled plasma-Mass spectrometry, ICP-MS  
168 (see details given in supplementary material). Analyzing REE fractionation in lateritic  
169 regoliths formed on granites potentially document on intensity of weathering processes  
170 (Nesbitt, 1979), but also on erosion distribution on landsurfaces carrying these regoliths.  
171 The Index Of Laterization (IOL) has been calculated for each sample analyzed (e.g., see  
172 Babechuk et al., 2014, after Schellmann classification of laterization grades in  
173 weathering profiles, 1994), with:

174

$$175 \quad \text{IOL} = 100 \times \left[ \frac{(\text{Al}_2\text{O}_3 + \text{Fe}_2\text{O}_3)}{(\text{SiO}_2 + \text{Al}_2\text{O}_3 + \text{Fe}_2\text{O}_3)} \right] \quad (1)$$

176

177 **4. Results**

178 4.1. Distribution, drainage, and incision of lateritic landsurfaces on granitoids

179 Three Lateritic landsurfaces formed on Panafrican granitic basement of  
180 Adamaoua highland are arranged in a stepping pattern on either side of a major drainage  
181 divide (Fig. 1b and 2a), which is delineated by more or less weathered recent late  
182 Neogene volcanic flow sequences (up to 2400 m a.s.l.; Fig. 1b), and the highest lateritic  
183 landsurfaces over granitoids (up to 1200 m a.s.l.). Drainage networks of Adamaoua  
184 highland are mostly organized in rectangular and parallel spatial patterns on granitoids,  
185 while more dendritic over volcanics (Fig. 2a). The northern domain is a relatively  
186 limited portion of the Adamaoua highland, which is drained by Faro and Vina Rivers,  
187 tributaries of Benoue and Logone fluvial networks that are main rivers of northern  
188 Cameroon (Fig. 1a). The southern domain of Adamaoua highland is gradually stepped  
189 (Fig. 2) from the highest to the lowest landforms (1450-1200 m to ~790 m a.s.l.; Figs.  
190 1b and 2a) that are shaped by the Sanaga river drainage network and its major tributary  
191 Djerem River (Figs. 1a and 2a). Long profiles of Djerem and major tributaries are  
192 punctuated by knickzones mostly pinned to lithological and/or structural discontinuities,  
193 delimiting concave shape stream lengths (Figs. 1c and 2a-b).

194 Regionally mapped-substrate (Fig. 1b) and our field observations on Panafrican  
195 Adamaoua highland highlight three lateritic landsurfaces (Figs. 2a, 3 and 4), which are  
196 bounded by erosional slopes and/or terraces (Figs. 2a) up to 100 m amplitude (Fig. 3),  
197 exposing granitic/gneissic bedrock. These three landsurfaces, i.e., upper, middle and  
198 lower (Figs. 3 and 4) are mantled by mixed or composite lateritic duricrusts and  
199 distinguished by their morphology (e.g., drainage network geometry, and hillslope  
200 shape). On Adamaoua, the lateritic landsurfaces are covered by a patchwork of clear  
201 and very dense humid savannas (Fig. 3a) typical of soudano-guinean climatic zones

202 (according to Aubréville, 1949). Sequences of kilometer wide multi-convex hills less  
203 than 50 m height (Fig. 3) recall similar landscapes described in Southern Nigeria  
204 (Rohdenburg, 1969; Fölster, 1969) in the guinean climatic zone.

205 On Adamaoua highland, the upper landsurface ranges between 1250 m a.s.l. and  
206 ~1150 m a.s.l. (Figs. 2a-b); it is a low-relief smoothly flattened lateritic etch-plain more  
207 or less dissected by V-shape shallow thalwegs with incision not exceeding 30 m height  
208 (Figs. 3b-c and 4a). The transition with the middle landsurface is outlined by erosional  
209 slopes up to ~ 100 m height over ~2 km (Figs. 3b and 4a) with outcropping granitic  
210 bedrock and/or preserved ferruginous carapaces or sandy mottled clays attesting of  
211 truncated profiles. Peripheral erosion of the etch-plain results in denuded (dismantled)  
212 slopes drained by short (first order) streams over average ~ 5% slope gradient (Figs. 2a-  
213 b). The etch-plain bears a thick lateritic regolith exposing up to ca. 2 m thick nodular  
214 ferricrete overlying pebbly lateritic and thick mottled clay layers (Figs. 5a-b).

215 Downstream, profiles of rivers draining the middle landsurface have gentle  
216 upward concave stream sections (Fig. 2b). This landsurface is a low-relief smooth hilly  
217 surface ranging from altitudes of 1100 m to 1050 m a.s.l. (Fig. 2a-b and 3b-c) formed in  
218 between erosional hillslopes of the upper etch-plain, and dissected into convex hills less  
219 than 1 km wide distributed (Figs. 3 and 4). A dendritic hydrographic network drains this  
220 landsurface (Figs. 2a and 4), which mostly exposes a “puzzle” of duricrusted regolith  
221 and ferruginized mottled clays (Fig. 5c). The middle landsurface is limited by erosional  
222 slopes drained by short (first order) streams over gentle slopes of ~ 3 % gradient (Figs.  
223 2b and 3b), which is paved by meter-sized disaggregated ferricrete blocks (Fig. 5d).

224 The lower landsurface is a very low-relief pediplain formed at altitude  $\leq$  1000 m  
225 a.s.l. (Figs. 3a-c) by coalescent pediments (Figs. 2a and 4b), mostly drained by a  
226 rectangular geometric network of linear tributaries of Djerem River system in southern

227 Adamaoua (Fig. 2a). This pediplain is covered by a more or less duricrusted regolith  
228 (Fig. 5e) on kilometer wide gentle slopes, which may also expose dismantled granitic  
229 blocks in area where erosion has totally stripped the lateritic regolith. Downslope, this  
230 landsurface may be covered by modern alluvial materials (Fig. 4b) similar as  
231 sedimentary fans of flood plains along main rivers (see also Chardon et al., 2018).  
232 Below erosional slopes (< 1000 m a.s.l.) this pediplain is shallowly dissected, with  
233 incisions not exceeding 10 m (Figs. 3b-c and 5f), while river streams have concave up  
234 profile (Fig. 2b).

235

#### 236 4.2. Regolith of lateritic landsurfaces on granitoids from Adamaoua highland

##### 237 4.2.1. Lateritic regolith of upper etch-plain landsurface

238 The lateritic regolith of this upper landsurface is mostly duricrusted by an Al-Fe  
239 rich nodular ferricrete. This ferricrete is made up of centimeter-sized dark-red nodules  
240 cemented in a yellowish matrix mixing iron oxy-hydroxides and clays crossed by  
241 vacuoles and studded by quartz grains (Figs. 6a) that typifies a moderately lateritized  
242 ferricrete (see #1 in Fig. 7). The duricrusted lateritic regolith of this landsurface may  
243 also encompass decimetric-sized rounded lateritic duricrusts of various facies including  
244 decimeter size relics of ferricrete and bauxite (Fig. 6b). These ferricrete and bauxitic  
245 relics have a paranodular to massive structure, respectively (Fig. 6c-d) showing pink  
246 patches embedded in a red Al-Fe rich ferruginous matrix crossed by voids filled by Al-  
247 oxyhydroxides that constitutes also strongly lateritised duricrusts (e.g., see #2 in Fig. 7).  
248 The bauxitic petrological relics are made up of centimeter size yellowish-grey patches  
249 in a yellow-reddish Al-Fe rich internodular matrix (Figs. 6e). Some other bauxite relics  
250 show a saprolitic texture, made up of a yellowish grey undifferentiated matrix studded  
251 with small (mm sized) quartz grains, which preserves the finely grained texture of the

252 granitic parent-rock (Fig. 6f). These bauxitic relics are strongly lateritized and very rich  
253 in aluminum (see #3 in Fig. 7). Bauxites and/or ferruginous bauxitic duricrusts relics are  
254 clearly differentiated from the encompassing nodular ferricrete on this pediplain (Fig.  
255 7).

256 Compared to trace elements and REE composition of the granitic parent rock, most of  
257 lateritic duricrusts and ferricretes of regolith formed on this landsurface are enriched in  
258 Ti, Cr, Cu, V, depleted in Mn, Y, Sr, Rb, Ba, Zn, Co, Pb, while Nb, Zr, Ga, Cu, Ni, Sc,  
259 Th, Hf, U, and Ta remain quite constant (Fig. 8a). Most of REE are depleted with higher  
260 variability in lateritic relics than in encompassing ferricrete, except some relics little  
261 enriched in LREE (Fig. 9a). Normalized to Upper Continental Crust (UCC)  
262 composition, lateritic relics have Ce/Ce\* comprised between 0.57-1.15 against 0.93-  
263 1.99 for the encompassing ferricrete, while Eu/Eu\* ranges from 0.97 to 1.45 compared  
264 to 0.9-1.29 for ferricrete (see also Table DR).

265

#### 266 4.2.2. Lateritic regolith of middle landsurface

267 Regolith of the middle landsurface is a protonodular ferruginous duricrust (see  
268 Tardy, 1997) composed of coalescent dark red nodules and concretions embedded in a  
269 clay-ferruginous matrix with yellowish frame of Fe-oxy-hydroxides studded by quartz  
270 grains and vacuolar voids (Fig. 10a; see also #4 in Fig. 7 for geochemical composition).  
271 The ferruginous duricrust also encompasses some detrital relics of older ferricrete (Fig.  
272 10b). This ferricrete has a paranodular to nodular structure with centimetric size purple-  
273 reddish nodules (1-2 cm sized) cerned by a brown rim and embedded in a clayey  
274 orange-ochre matrix (Fig. 10c-d). These ferricretes are comparable to the nodular  
275 ferricrete of the upper landsurface (see # 5 and #1 in Fig. 7). Most iron duricrusts of the  
276 middle landsurface are however less ferruginous but as aluminous as duricrusts of the

277 upper landsurface and rather moderately lateritised (Fig. 7). Note that analyses obtained  
278 on detrital ferricrete relics encompassed in duricrusted regolith of that middle  
279 landsurface clearly plotted on the (Fe<sub>2</sub>O<sub>3</sub>-Kaolinite) axis (Fig. 7).  
280 Most of lateritic duricrusts and ferricrete formed on this landsurface are enriched in Cr,  
281 Cu, V, Pb, Ta, depleted in Mn, P, Y, Sr, Rb, Ba, Zn, Ni, Co, while Ti, Nb, Zr, Ga, Sc,  
282 Th, Hf, and U, remain quite constant (Fig. 8b). Most of REE are depleted, except some  
283 lateritic relics little enriched in LREE, e.g., Ce, Pr, Nd and Sm, while some  
284 encompassing ferricrete have higher HREE, i.e., Tm, Yb and Lu (Fig. 9b). Normalized  
285 to UCC composition, lateritic relics have Ce/Ce\* comprised between 0.78 and 1.15  
286 against 0.82-1.18 for the encompassing ferricrete, while Eu/Eu\* ranges from 1.07 to  
287 1.34 compared to 0.84-1.21 for ferricrete (see also Table DR).

288

#### 289 4.2.3. Lateritic regolith of lower pediplain landsurface

290 The regolith of this landsurface exposes more or less weathered laterites, either  
291 saprolitic relics (Fig. 11a), or more or less duricrusted mottled clays (Fig. 11b), which  
292 are only kaolinized (see #6-7 in Fig. 7), and ferricretes. These ferricretes have a  
293 paramodular to nodular structure, composed of large purple-reddish ferruginous nodules  
294 with a brown peripheral rim of goethite (Figs. 11c-d), and often preserve centimeter-  
295 sized saprolite and/or mottled clays, which are crossed by a tubular porosity lined with  
296 secondary brown coatings of goethite mainly (Fig. 11d). Ferricretes of this pediplain are  
297 rich in Fe oxy-hydroxides and kaolinite (see #8 in Fig. 7) comparable to ferricretes of  
298 the middle landsurface. The highly variable IOL index of this pediplain (Fig. 7) reflects  
299 differentially eroded (truncated) profiles exposing saprolite (Fig. 11a), mottled clays  
300 (Fig. 11b), and/or moderately lateritised duricrusts (Figs. 11c-d), but which IOL is  
301 comparable to that of lateritic duricrusts of upper and middle landsurfaces (Fig. 7).

302 Most of lateritic duricrusts of this pediplain are enriched in Cr, Cu, V, U, depleted in Ti,  
303 Mn, P, Y, Sr, Rb, Ba, Zn, Co, while Nb, Zr, Ga, Sc, Th, Hf, Ta and Yb, remain quite  
304 constant (Fig. 8c). Note that Cu and Ta are highly depleted in lateritic relics. Most of  
305 REE are highly depleted, except some HREE, i.e., Tm, Yb and Lu, with concentration  
306 comparable to parent rock composition (Fig. 9c). Ce/Ce\* varies from 0.57 to 5.08 while  
307 Eu/Eu\* ranges from 0.73 to 1.25 (see also Table DR).

## 308 **5. Discussion**

### 309 5.1. Petro-geochemical differentiation of lateritic regoliths on Panafrican of Adamaoua

310 Although quite similar trace and REE normalized patterns of regolith from the  
311 three landsurfaces (Figs. 8 and 9), some differences and specificities can be noted.  
312 Lateritic duricrusted regolith of the upper etch-plain landsurface are the most lateritised  
313 and the richest in Al<sub>2</sub>O<sub>3</sub>, Fe<sub>2</sub>O<sub>3</sub>, Ti and Cr (Figs. 7, 8 and 12), Nb and Ta (Fig. 13a-b)  
314 that mostly typify Al-Fe rich duricrusts and bauxites such as those described in West  
315 Africa (e.g., Boulangé, 1984; Sawadogo, 2021). Lateritic duricrusted regolith  
316 (ferricretes) of the middle landsurface is rather less aluminous but as ferruginous and  
317 richer in Cu, V and Ga (Figs. 8, 12 and 13c-d). Lateritic relics encompassed in the  
318 ferruginous duricrust of this landsurface are also likely composed of a mixed kaolinite  
319 and Fe-oxy-hydroxides as suggested by the plots aligned on the mixture line Fe<sub>2</sub>O<sub>3</sub> -  
320 Kaolinite (Fig. 7) that also typifies regolith of intermediate etch-plain type landsurfaces  
321 of Central and West Africa (Boulangé, 1984; Roquin et al., 1990; Beauvais and Roquin,  
322 1996; Beauvais, 1999; Sawadogo, 2021). According to some differences in granitic  
323 parent rocks geochemistry Zr and Ti are differently correlated in lateritic duricrusted  
324 regoliths of the three landsurfaces (Fig. 13e). Although Zr concentrations of ferricretes  
325 and lateritic duricrusts (relics) are comparable, Ti amounts in lateritic regolith of the  
326 upper etched lateritic landsurface are higher than in middle and lower landsurfaces

327 (Figs. 13e). Ferricretes and lateritic relics of the upper landsurface are the most  
328 lateritised (higher IOL) and have also higher Ti and Nb, but lower Zr/Ti and Nb/Y ratio  
329 than ferricretes and lateritic relics of the middle and lower landsurfaces (Figs. 13a-13e-f  
330 and Figs. 14a-b). A slight increase in Zr and Ti (and correlatively, Zr/Ti) is noted from  
331 the granitic bedrocks to lateritic duricrusts of middle and lower landsurfaces (Figs. 13-e-  
332 f) reflecting lithological dependence. Though Zr and Ti also increase together from the  
333 bedrock to ferricrete of upper landsurface, Zr of lateritic relics in regolith of this  
334 landsurface shows poor relation to bedrock while Ti clearly increases (Figs. 13e-f).  
335 These results underline the allochthonous nature of some lateritic duricrusts and  
336 ferricretes, and more particularly the bauxitic nature of most highly lateritized relics  
337 from duricrusted regolith of the upper etched landsurface. Ferricretes and lateritic relics  
338 of regolith of the three landsurfaces show obvious differences in V, Zr and Ti reflecting  
339 geochemical variations of granitic parent rocks (Figs. 12, 13c and 13e-f) but also  
340 differences of laterization gradient (Fig. 7) that may have perturbed the lithological  
341 dependence. It was previously shown in West Africa that lateritic crusts potentially  
342 loose geochemical relation to parent rock as the most lateritized and old they are (e.g.,  
343 Tardy, 1997).

344 Although REE are highly depleted in most of lateritic duricrusted regolith (Fig. 9), some  
345 fractionation occur in lateritic regolith of the first two landsurfaces (Figs. 9a-b), with  
346 higher Eu/Eu\* and Th, but lower (Gd/Yb)<sub>N</sub>, and HREE in duricrusted lateritic regolith  
347 of middle landsurface compared to regolith of upper and lower landsurfaces (14b to  
348 14d). That possibly reflects different redox conditions in laterization processes of the  
349 three landsurface-regolith systems (Braun et al., 1993; Boulangé and Colin, 1994; see  
350 also Brown and Helmke, 2003). Regoliths of the lower landsurface (pediplain type) are  
351 less lateritised and more siliceous (Fig. 7) and have a little more variable trace and REE



352 composition (Figs. 8c and 9c). They are less aluminous, ferruginous and titaniferous,  
353 better retain U and have comparable content in Cr, V, Cu, Nb, Ta and Ga content (Figs.  
354 8, 9, 12 and 13). Lateritic regolith of this landsurface have also lower Ti, Nb, Th,  
355 Eu/Eu\* and  $(\text{Gd/Yb})_N (< 1)$  but are a little richer in HREE, and Y compared to regolith  
356 of the first two landsurfaces (Figs. 14a to 14d). That suggests residual primary HREE  
357 carriers like zircons (Gromet and Silver, 1983; Murali et al., 1983; Fig. 14a) or some  
358 relics of poorly weathered Fe-Mg primary minerals like biotite and/or hornblende in  
359 kaolinite rich weathering matrices that also take up HREE (see Nesbitt, 1979).  
360 Variations in Ce/Ce\* in ferricretes and lateritic duricrusts of landsurfaces regolith also  
361 reflect variable redox conditions (Braun et al., 1993; Beauvais, 1999; Brown and  
362 Helmke, 2003; Babechuk et al., 2014) of different laterization intensity (see IOL  
363 gradient in Fig. 7). The petro-geochemical patterns of lateritic duricrusts and ferricretes  
364 of upper and middle landsurfaces typify regoliths of etch-plains (Thomas, 1994;  
365 Beauvais, 1999), while differently lateritised regoliths of the lower landsurface are  
366 closer to those of glaciais/pediaplains from West Africa (Roquin et al., 1990; Sawadogo,  
367 2021).

368

## 369 5.2. Lateritic landscape differentiation upon Panafrican basement of Adamaoua

370 Our results describe landscape-regolith associations with differentiation of three  
371 stepped lateritic landsurfaces on Adamaoua highland. The upper and middle  
372 landsurfaces are covered by composite lateritic duricrusted regolith encompassing  
373 duricrusted bauxite and ferricretes, which recall lateritic regolith of bauxitic and/or  
374 ferruginous intermediate etch-plain type surfaces described in West Africa (e.g.,  
375 Grandin, 1976; Thomas, 1994; Grimaud et al., 2015; Chardon et al., 2018; see also  
376 Chardon, 2023), or in south-eastern Central African Republic (e.g., Beauvais and

377 Roquin, 1996; Beauvais, 1999) in a certain extent. Old lateritic duricrusts of  
378 intermediate etch-plain type have been also previously described by Frisch (1978).  
379 These lateritic duricrusts including bauxite portray a former lateritic regolith that  
380 covered more widely the Adamaoua landscape similarly as the old lateritic regolith of  
381 the West African Eocene African Surface (Tardy and Roquin, 1998; Chardon et al.,  
382 2006; Grimaud et al., 2015; see also Grandin, 1976, and Sawadogo, 2021).  
383 Geomorphological landmarks of the continental scale African Surface (e.g., Burke and  
384 Gunnell, 2008) have been previously recognized and described in West Africa (see  
385 Michel, 1973; Grandin and Thiry, 1983), South Africa (Partridge and Maud, 1987) and  
386 Nigeria (Valeton, 1991; Schwarz, 1997; Becker, 1992). This major continental  
387 paleosurface was also recently further characterized and dated in West Africa (Beauvais  
388 et al., 2008; Beauvais and Chardon, 2013), and in Eastern Africa (Perelló et al., 2020).  
389 Lateritic Regolith typifying the African Surface type in Adamaoua has formed under  
390 humid climatic conditions since Eocene, i.e., the onset of mantle source basaltic  
391 volcanism southwest of Adamaoua highland (e.g., Fosso et al., 2005; Moundi et al.,  
392 2007). Early Eocene volcanic dynamic sustained regional scale epirogeny that led to  
393 topographic uplift of Western and Adamaoua Highlands (Morin, 1987, 1989), and the  
394 Jos high plateau in Nigeria (Valeton, 1991; Becker, 1992) with correlative regional base  
395 level adjustments. In Adamaoua like in Nigeria, amplified regional orography and  
396 increasing relief also allowed maintaining humid climatic regimes and efficient drainage  
397 that enhanced the geochemical rock weathering and regolith formation and evolution  
398 (mostly degradation) of former Eocene etch-plain landsurface. The ( $\text{SiO}_2$  -  $\text{Al}_2\text{O}_3$  -  
399  $\text{Fe}_2\text{O}_3$ ) compositions of lateritic regolith show on-going but quite differentiated  
400 geochemical evolution with a clear differentiated laterization gradient of the duricrusted  
401 regolith from the upper to the lower landsurface (Fig. 7). That reflects a dynamical

402 landform-regolith differentiation under persistent per-humid climatic regime most of  
403 Cenozoic times even if drying in late Neogene (see Bilobe et al., 2021) may have  
404 possibly affected landsurface erosion pattern. The strong laterization ( $IOL > 85$ ; Fig. 7)  
405 of the upper landsurface regolith brings it closer to the intermediate etch-plain type  
406 regolith (see also Fritsch, 1978) from West Africa (e.g., Sawadogo, 2021). Likewise, the  
407 regolith composition of the lower landsurface (Fig. 7) is very close to that of the high  
408 glaciais pediplain from West Africa (Sawadogo, 2021).

409 Mid-Miocene basaltic and andesitic outpourings (Marzoli et al., 2000) post-date  
410 the establishment of the upper and middle landsurfaces (Fig. 2a), while predating that of  
411 the lower landsurface. The northeastern part of Djerem watershed around the Tchabal  
412 Nganha (Fig. 2a) has been uplifted during Late Neogene volcanic activity (Gouthier et  
413 al., 1974; Halliday et al., 1988) but it remains difficult to measure this uplift on  
414 knickpoints of the upslope long profiles of Djerem and uppermost tributaries (Figs. 1b-  
415 c) to evaluate effects on landscape erosion and river incision patterns. Marked  
416 knickpoints also occur on long profiles of rivers flowing only on granitoid basement in  
417 the southwestern part of Djerem watershed and are mostly pinned to litho-structural  
418 discontinuities (Fig. 1b-c and 2a-b). Though late Neogene volcanic uplift is not  
419 measurable, very discrete short wavelength convexities are depicted locally in some  
420 sections of River long profiles, e.g., at 150-180 km between consecutive knick-points of  
421 Djerem River incising the lower pediplain landsurface (Fig. 1c and 2b). However, River  
422 long profiles of Djerem and its tributaries mostly show upward concave shape stream  
423 segments bounded by knick-zones pinned to lithological discontinuities (Figs. 1c and  
424 2b). Streams with concave morphology have adjusted to local base levels attesting of  
425 equilibrium state that also recall river incision pattern of West African landscapes (e.g.,  
426 Grimaud et al., 2014). Most River long profiles have first adapted to the inherited horst

427 topography of Adamaoua highland much before Neogene uplift. Moderate incision of  
428 the upper landsurface (Figs. 2a, 3b-c and 4a) typifies low-relief paleo-landsurface  
429 (Partridge and Maud, 1987) and/or subdued morphologies (McFarlane, 1976;  
430 Widdowson, 1997) recalling also smooth etch-plains south of the sahelian zone of  
431 Africa (Grandin, 1976; Thomas, 1994; Chardon et al., 2018; Chardon, 2023). Low  
432 incision and long-lasting humid climatic conditions precluded from complex slope  
433 erosion processes that have been often described in relief inversion context of Soudan-  
434 Sahelian tropical regions under more contrasted climatic regimes (e.g., Pain and Ollier,  
435 1995; Butt and Bristow, 2013; Chardon et al., 2018). Instead, Guinean to Soudano-  
436 Guinean per-humid environments prevailing as far as early Cenozoic in southern  
437 Adamaoua (Martin, 1970; Morin 1989; see also Burke and Gunnell, 2008) have mostly  
438 instigated the geochemical degradation and erosion processes (dismantling) of early  
439 formed bauxitic and ferricrete mantled-paleo-landsurfaces similarly as those described  
440 in West Africa (see Sawadogo, 2021) or in Eastern Central Africa (Beauvais and  
441 Roquin, 1996; Beauvais, 2009).

442         Though Adamaoua highland first results from regional epirogeny created by  
443 Eocene volcanic geodynamics, lateritic regolith of stepped landsurfaces evolved under  
444 persistent tropical per-humid climatic regime over most of Cenozoic times that is the  
445 reversed climatic evolution of West Africa (Morin, 1989; Burke and Gunnell, 2008; see  
446 also Chardon, 2023). Gradually stepped surfaces evolved under a humid climate typical  
447 of rainforests environments whereby a subdued regional incision/denudation precludes  
448 relief inversions of abandoned older landsurfaces as often observed in West Africa (see  
449 Chardon, 2023). Combined geodynamic and climatic factor have favored long-lasting  
450 weathering and degradation of former lateritic landsurfaces under slow erosion regime  
451 typical of cratonic regions submitted to less than 10 m/Myr erosion rates (Beauvais and

452 Chardon, 2013; Chardon et al., 2018). Such tectonic and climatic conditions are  
453 required for efficient laterization process and differentiated landscape structuration in  
454 humid tropical regions (e.g., Fölster, 1969; Valetton, 1991). Even if late Neogene  
455 volcanic uplift effect on landscape evolution cannot be totally excluded, this is not  
456 measurable. However, local topographic changes may have influenced distribution and  
457 frequency of rainfalls, and potentially led to further geochemical degradation of lateritic  
458 regoliths on Adamaoua highlands. Further detailed geomorphological studies combined  
459 with geochronological dating of lateritic surfaces and their duricrusts (e.g., (U-Th)/He-  
460  $^4\text{He}/^3\text{He}$  dating of iron oxy-hydroxides; see Vasconcelos et al., 2013; Monteiro et al.,  
461 2018; Heller et al., 2022), which formed on both granitoids and volcanic rocks  
462 (including  $^{40}\text{Ar}-^{39}\text{Ar}$  dating of these as well), would be however required to better  
463 constrain the impact and timing of major geodynamic and climatic weathering/erosion  
464 processes and their interactions on Adamaoua landscapes over Cenozoic.

465

## 466 **6. Conclusion**

467 Three stepped lateritic landsurfaces have been formed upon Pan-African  
468 basement of Adamaoua highland as smooth etch-plain type surfaces with subdued  
469 hillslopes and flattened pediplain separated the one to other by more or less rugged  
470 erosional slopes. Lateritic regolith of the upper and middle landsurfaces encompasses  
471 older lateritic duricrusts (bauxite and ferricrete) inherited from presumably Eocene  
472 bauxitic and intermediate etch-plain type paleosurfaces, which have slowly evolved  
473 mostly by geochemical degradation owing to long-lasting humid climatic conditions  
474 since Eocene epirogenic uplift of Adamaoua. These old lateritic duricrusts are  
475 petrologic signatures of former regolith that widely covered the Panafrican basement of  
476 Adamaoua highland and can be compared to similar regolith of the continental scale

477 Paleogene African surface described in West and East Africa. Geochemical  
478 compositions of lateritic regolith formed on each landsurface are distributed between  
479 aluminous, ferruginous and Si-Al poles with a noticeable gradient of laterization (IOL)  
480 and differential fractionation patterns of trace elements (mostly, Ti, Cr, V, Zr, Nb, Th,  
481 Y, Ta and Ga) and REE (i.e., Ce\*, Eu\*, Gd<sub>N</sub>/Yb<sub>N</sub>, and HREE) that allow a better  
482 distinction of regolith of these three landsurfaces. Mid-Miocene basalt/andesite  
483 outpourings post-date the upper and middle etch-plain landsurfaces while pre-dating  
484 formation of the lower pediplain. Late Neogene volcanics extrusions through major  
485 structures across the PanAfrican basement have locally uplifted Adamaoua landscape,  
486 that potentially constrained laterization and erosion/degradation processes of  
487 landsurfaces, even if uplift is not measurable. Landsurface-regolith mostly formed on an  
488 inherited horsts topography under persistent per-humid climates at least from ~ mid-  
489 Eocene. Possible late Neogene drying has diversely affected landscape as suggested by  
490 differential erosion fingerprints and patchwork of more or less eroded or stripped  
491 lateritic regolith of the lower pediplain.

492

### 493 **Acknowledgments**

494 This work is a contribution to the JEAJ project “MORPHOCAM” (2021-2023) funded  
495 by the French Research Institute for the sustainable Development (IRD). Financial  
496 support was also first provided by APIC annual programs (2019-2020) from the  
497 « Centre Européen de Recherche et d'Enseignement des Géosciences de  
498 l'Environnement » (CEREGE). MNM was supported by long-lasting scientific stays  
499 (MLD) granted by IRD for his collaborative researches at Cerege, Aix Marseille  
500 Université, OSU Pytheas, France. We acknowledge two anonymous reviewers and the

1 handling editor for their criticisms and remarks that contribute to improve our  
2 manuscript.

#### 4 **References**

5 Aubréville, A., 1949. *Climats, forêts et désertification de l'Afrique tropicale*. Société  
6 d'Éditions géographiques maritimes et coloniales, Paris.

7 Babechuk, M.G., Widdowson, M., Kamber, B.S., 2014. Quantifying chemical intensity  
8 and trace element release from two contrasting profiles, Decan Traps, India.  
9 *Chemical Geology* 365, 56-75.

10 Beauvais, A., 1999. Geochemical balance of lateritization processes and climatic  
11 signatures in weathering profiles overlain by ferricretes in Central Africa. *Geochim.*  
12 *Cosmochim. Acta* 63, 3939–3957.

13 Beauvais, A., 2009. Ferricrete biochemical degradation on the rainforest savannas  
14 boundary of Central African Republic. *Geoderma*, 150, 379–388.

15 Beauvais, A., Chardon, D., 2013. Modes, tempo, and spatial variability of Cenozoic  
16 cratonic denudation: The West African example. *Geochemistry, Geophysics,*  
17 *Geosystems* 14, 1590-1608.

18 Beauvais, A., Roquin, C., 1996. Petrological differentiation patterns and geomorphic  
19 distribution of ferricretes in Central Africa. *Geoderma* 73, 63–82.

20 Beauvais, A., Ruffet, G., Hénocque, O., Colin, F., 2008. Chemical and physical erosion  
21 rhythms of the West African Cenozoic morphogenesis: the <sup>39</sup>Ar-<sup>40</sup>Ar dating of  
22 supergene K-Mn oxides. *Journal of Geophysical Research: Earth Surface* 113.

23 Becker, A., 1992. A time-space model for the genesis of Early Tertiary laterites from  
24 the Jos Plateau, Nigeria. *Journal of African Earth Sciences (and the Middle East)*  
25 15, 265–269.

26 Bilobe, J. A., Feist-Burkhardt, S., Eyong, J. T., Samankassou, E., 2021. Biostratigraphy  
27 of Cretaceous-Neogene sedimentary infill of the Mamfe basin, southwest  
28 Cameroon: Paleoclimate implication. *Jour. Afr. Earth Sci.* 182, 104279.

29 Bonnet, N.J., Beauvais, A., Arnaud, N., Chardon, D., Jayananda, M., 2016. Cenozoic  
30 lateritic weathering and erosion history of Peninsular India from  $^{40}\text{Ar}/^{39}\text{Ar}$  dating  
31 of supergene K–Mn oxides. *Chem. Geol.* 446, 33-53.

32 Boulangé, B., 1984. Les formations bauxitiques latéritiques de Côte d’Ivoire. Les faciès,  
33 leur transformation, leur distribution et l’évolution du modelé. *Travaux et*  
34 *Documents de l’ORSTOM*, 175, pp. 345.

35 Boulangé, B., Colin, F., 1994. Rare-earth element mobility during conversion of  
36 nepheline syenite into lateritic bauxite at Passa Quatro, Minas Gerais, Brazil. *Appl.*  
37 *Geochem.* 9, 701–711.

38 Braun, J.J., Pagel, M., Herbillon, A., Rosin, C., 1993. Mobilization and redistribution of  
39 REEs and thorium in syenitic lateritic profile: a mass balance study. *Geochim.*  
40 *Cosmochim. Acta* 57, 4419–4434.

41 Brown, D.J., Helmke, P.A., 2003. Robust geochemical indices for redox and weathering  
42 on a granitic laterite landscape in Central Uganda. *Geochim. Cosmochim. Acta* 67  
43 (15), 2711–2723.

44 Burke, K., 2001. Origin of the Cameroon line of volcano-capped swells. *The Journal of*  
45 *Geology* 109, 349-362.

46 Burke, K., Gunnell, Y., 2008. The African erosion surface: a continental-scale synthesis  
47 of geomorphology, tectonics, and environmental change over the past 180 million  
48 years. *Geological Society of America, Memoir* 201 1 - 66.

49 Butt, C.R.M., Bristow, A.P.J., 2013. Relief inversion in the geomorphological evolution  
50 of sub-Saharan West Africa. *Geomorphology* 185, 16–26.



51 Chardon, D., 2023. Landform-regolith patterns of Northwestern Africa: Deciphering  
52 Cenozoic surface dynamics of the tropical cratonic geosystem. *Earth-Science*  
53 *Reviews* 242,104452.

54 Chardon, D., Chevillotte, V., Beauvais, A., Grandin, G., Boulangé, B., 2006. Planation,  
55 bauxites and epeirogeny: One or two paleosurfaces on the West African margin?  
56 *Geomorphology* 82, 273-282.

57 Chardon, D., Grimaud, J.-L., Beauvais, A., Bamba, O., 2018. West African lateritic  
58 pediments: Landform-regolith evolution processes and mineral exploration pitfalls.  
59 *Earth-Science Reviews* 179, 124-146.

60 Colin, F., Beauvais, A., Ruffet, G. & Hénocque, O. 2005. First  $^{40}\text{Ar}/^{39}\text{Ar}$   
61 geochronology of lateritic manganiferous pisolites: Implications for the Palaeogene  
62 history of a West African landscape. *Earth and Planetary Science Letters*, 238, 172–  
63 188.

64 Dautria, J.-M., Girod, M., 1986. Les enclaves de lherzolite à spinelle et plagioclase du  
65 volcan de Dibi (Adamaoua, Cameroun) : des témoins d'un manteau supérieur  
66 anormal. *Bulletin de minéralogie* 109, 275-288.

67 Fitton, J.G., 1980. The Benue trough and Cameroon line - a migrating rift system in  
68 West Africa. *Earth and Planetary Science Letters* 51, 132–138.

69 Fölster, H., 1969. Late Quaternary erosion in SW-Nigeria. *Bull. Ass. Sén. Et. Quat.*  
70 *Ouest Afr.* 21, 29–35.

71 Fosso, J., Ménard, J.-J., Bardintzeff, J.-M., Wandji, P., Tchoua, F. M., Bellon, H., 2005.  
72 Lavas from the Mount Bangou area: A first Eocene volcanic episode with  
73 transitional affinities of Cameroon Line. *C. R. Géoscience* 337(3), 315-325.

74 Frisch, P. 1978. Chronologie relative des formations cuirasses, et analyse géographique  
75 du cuirassement au Cameroun. *Travaux et Documents de Géographie Tropicale*,

76 CEGET, Géomorphologie des reliefs cuirassés dans les pays tropicaux chauds et  
77 humides, 33, 114-132.

78 Grandin, G., 1976. Aplanissements cuirassés et enrichissement des gisements de  
79 manganèse dans quelques régions d'Afrique de l'Ouest, Mémoire ORSTOM.  
80 ORSTOM, Paris, 1 - 275.

81 Grimaud, J.-L., Chardon, D., Beauvais, A., 2014. Very long-term incision dynamics of  
82 big rivers. *Earth. Planet. Sci. letters* 405, 74-84.

83 Grimaud, J.-L., Chardon, D., Metelka, V., Beauvais, A., Bamba, O., 2015. Neogene  
84 cratonic erosion fluxes and landform evolution processes from regional regolith  
85 mapping (Burkina Faso, West Africa). *Geomorphology* 241, 315–330.

86 Gromet, P.L., Silver, L.T., 1983. Rare earth element distributions among minerals in a  
87 granodiorite and their petrogenetic implications. *Geochim. Cosmochim. Acta* 47(5),  
88 925–939.

89 Guillocheau, F., Chelalou, R., Linol, B., Dauteuil, O., Robin, C., Mvondo, F., Callec,  
90 Y., Colin, J-P., 2015. Cenozoic landscape evolution in and around the Congo basin:  
91 Constraints from sediments and planation surfaces. In M.J. de Wit et al. (eds),  
92 *Geology and Resource potential of the Congo basin*, Regional Geology Reviews.  
93 Springer-Verlag. doi:10.1007/978-3-642-29482-2\_14.

94 Halliday, A.N., Dickin, A.P., Fallick, A.E. and Fitton, J.G., 1988. Mantle dynamics: a  
95 Nd, Sr, Pb and O isotopic study of the Cameroon line volcanic chain. *J. Petrol.*  
96 29,181-211.

97 Heller, B.M., Riffel, S.B., Allard, T., Morin, G., Roig, J-Y., Couëffé, R., Aertgeerts, G.,  
98 Derycke, A., Ansart, C., Pinna-Jamme, R., Gautheron, C., 2022. Reading the  
99 climate signals hidden in bauxite. *Geochim. Cosmochim. Acta* 323, 40-73.

100 Jean, A., Beauvais, A., Chardon, D., Arnaud, N., Jayananda, M., Methe, P-E., 2020.  
101 Weathering history and landscape evolution of Western Ghats (India) from  
102  $^{40}\text{Ar}/^{39}\text{Ar}$  dating of supergene K–Mn oxides. *J. Geol. Soc.* 177, 523-536.

103 Jorgensen, G.J., Bosworth, W., 1989. Gravity modeling in the Central African Rift  
104 System, Sudan: Rift geometries and tectonic significance. *Journal of African Earth*  
105 *Sciences (and the Middle East)* 8, 283–306.

106 Marques, K.P., dos Santos, M., Peifer, D., da Silva, C.L., Vidal-Torrado, P., 2021.  
107 Transient and relic landforms in a lithologically heterogeneous post-orogenic  
108 landscape in the intertropical belt (Alto Paranaíba region, Brazil). *Geomorphology*  
109 391, 107892.

110 Martin, D., 1970. Quelques aspects des zones de passage entre surfaces d’aplanissement  
111 du Centre-Cameroun. *Cah. ORSTOM, sér. Pédol.*, VIII, 219–229.

112 McFarlane, M.J., 1976. *Laterite and landscape*. Academic Press.

113 Marzoli, A., Piccirillo, E.M., Renne, P.R., Bellieni, G., Iacumin, M., Nyobe, J.B.,  
114 Tongwa, A.T., 2000. The Cameroon volcanic line revisited: Petrogenesis of  
115 continental basaltic magmas from lithospheric and asthenospheric mantle sources.  
116 *Journal of Petrology* 41(1), 87-109.

117 Michel, P., 1973. Les bassins des fleuves Sénégal et Gambie : étude géomorphologique.  
118 *Revue Géographique de l'Est*, 237-242.

119 Momo Nouazi, M., Beauvais, A., Tematio, P., Yemefack, M., 2020. Differentiated  
120 Neogene bauxitization of volcanic rocks (western Cameroon): Morpho-geological  
121 constraints on chemical erosion. *Catena* 194, 104685.

122 Monteiro, H.S., Vasconcelos, P.M.P., Farley, K.A., Lopes, C.A.M., 2018. Age and  
123 evolution of diachronous erosion surfaces in the Amazon: Combining (U-Th)/He  
124 and cosmogenic  $^3\text{He}$  records. *Geochim. Cosmochim. Acta* 229, 162-183.

125 Moreau, C., Regnault, J.-M., D6ruelle, B. and Robineau, B., 1987. A new tectonic  
126 model for the Cameroon Line. *Tectonophysics* 139, 317-334.

127 Morin, S., 1987. Cuirasses et reliefs de l'Ouest Cameroun. Laboratoire de  
128 Géomorphologie du CEGET/CNRS, 33405 Talence France 107 - 118.

129 Morin, S., 1989, Hautes terres et bassins de l'ouest du Cameroun : Étude  
130 géomorphologique. Ph.D. thesis, Talence, University of Bordeaux 3, 1190 p.

131 Moundi, A., Wandji, P., Bardintzeff, J.-M., Ménard, J.-J., Okomo Atouba, L.C., Reusser,  
132 E., Bellon, H., and Tchoua, M.F., 2007, Les basaltes éocènes à affinité  
133 transitionnelle du plateau Bamoun, témoins d'un réservoir mantellique enrichi sous  
134 la ligne volcanique du Cameroun: *C. R. Geoscience* 39, 396–406,  
135 doi:10.1016/j.crte.2007.04.001.

136 Murali, A. V., Parthasaraty, R., Mahadevan, T. M., Sankar Das M., 1983. Trace  
137 elements characteristics, REE patterns and partition coefficients of zircons from  
138 different geological environments. A case study on Indian zircons. *Geochim.*  
139 *cosmochim. Acta* 47, 2047-2052.

140 Nesbitt, H. W., 1979. Mobility and fractionation of rare earth elements during  
141 weathering of a granodiorite. *Nature* 279, 206-210.

142 Ngako, V., Affaton, P., Nnange, J.M., Njanko, T., 2003. Pan-African tectonic evolution  
143 in central and southern Cameroon: transpression and transtension during sinistral  
144 shear movements. *Journal of African Earth Sciences* 36, 207-214.

145 Ngako, V., Njonfang, E., Aka, F.T., Affaton, P., Nnange, J.M., 2006. The North–South  
146 Paleozoic to Quaternary trend of alkaline magmatism from Niger–Nigeria to  
147 Cameroon: complex interaction between hotspots and Precambrian faults. *Journal*  
148 *of African Earth Sciences* 45, 241–256.

149 Njonfang, E., Nono, A., Kamgang, P., Ngako, V., Tchoua, F.M., 2011. Cameroon Line  
150 alkaline magmatism (central Africa): a reappraisal. *Geol. Soc. Am. Spec. Pap.* 478,  
151 173–191. [https://doi.org/10.1130/2011.2478\(09\)](https://doi.org/10.1130/2011.2478(09)).

152 Nkouandou, O.F., Bardintzeff, J.-M., Fagny, A.M., 2015. Sub-continental lithospheric  
153 mantle structure beneath the Adamawa plateau inferred from the petrology of  
154 ultramafic xenoliths from Ngaoundere (Adamawa plateau, Cameroon, Central  
155 Africa). *Journal of African Earth Sciences* 111, 26-40.

156 Nono, A., Déruelle, B., Demaiffe, D., and Kambou, R., 1994, Tchabal Nganha volcano  
157 in Adamawa (Cameroon): Petrology of a continental alkaline lava series: *Journal of*  
158 *Volcanology and Geothermal Research* 60, 147- 178. doi:10.1016/0377-  
159 0273(94)90066-3.

160 Pain, C.F., Ollier, C.D., 1995. Inversion of relief- a component of landscape evolution.  
161 *Geomorphology* 12(2), 151-165.

162 Partridge, T.C. & Maud, R.R. 1987. Geomorphic evolution of southern Africa since the  
163 Mesozoic. *South African Journal of Geology*, 90, 179–208.

164 Perelló, J., Brockway, H., García, A., 2020. A minimum Thanetian (Paleocene) age for  
165 the African Surface in the Eritrean highlands, Northeast Africa. *Journal of African*  
166 *Earth Sciences* 164, 103782.

167 Poudjom-Djomani, Y.H., Diament, M., Wilson, M., 1997. Lithospheric structures  
168 across the Adamawa plateau (Cameroon) from gravity studies, *Tectonophysics* 273,  
169 317-327.

170 Retallack, G.J., 2010. Lateritization and bauxitization events. *Economic Geology* 105,  
171 655–667.

172 Rohdenburg, H., 1969. Hangpedimentation and klimawechsel als wichtigste faktoren  
173 der flächen- und stufenbildung in den wechselfeuchten tropen an beispielen aus

174 Westafrica, besonders aus dem schichtstufenland Südost-Nigerias. Göttinger  
175 Bodenkdl. Ber. 10, 57–133.

176 Roquin, C., Freyssinet, P., Zeegers, H., Tardy, Y., 1990. Element distribution patterns in  
177 laterites of southern Mali: consequence for geochemical prospecting and mineral  
178 exploration. *Appl. Geochem.* 5(3), 303-315.

179 Sawadogo, B., 2021. Cartographie des régolites du Centre-Nord Burkina Faso (Aafrique  
180 de l'Ouesr) : Implications fondamentales et appliquées. PhD Thesis, Université de  
181 Ouagadougou, Burkina Faso, pp. 235.

182 Sawadogo, B., Bamba, O., Chardon, D., 2020. Landform-regolith mapping in the West  
183 African context. *Ore Geology Reviews* 103782.

184 Schellmann, W., 1994. Geochemical differentiation in laterite and bauxite formation.  
185 *Catena* 21, 131–143.

186 Schwarz, T., 1997. Distribution and genesis of bauxite on the Mambilla Plateau. SE  
187 Nigeria. *Applied geochemistry* 12, 119–131.

188 Segalen, P., 1967. Les sols et la géomorphologie du Cameroun. Cahiers ORSTOM.  
189 Série Pédologie, 5 (2), 137-187.

190 Tardy, Y., 1997. Petrology of Laterites and Tropical Soils. Balkema. Balkema,  
191 Rotterdam, The Netherlands.

192 Tardy, Y., Roquin, C., 1998. Dérive des continents paléoclimats et altérations  
193 tropicales. Ed. BRGM, Orléans 1, 1 - 473.

194 Taylor, R.G., Howard, K.W.F., 1998. Post-Palaeozoic evolution of weathered  
195 landsurfaces in Uganda by tectonically controlled deep weathering and stripping.  
196 *Geomorphology* 25, 173–192. [https://doi.org/10.1016/S0169-555X\(98\)00040-3](https://doi.org/10.1016/S0169-555X(98)00040-3)

197 Thomas, M.F., 1994. Geomorphology in the Tropics – A Study of weathering and  
198 denudation in low latitudes. Wiley & Sons, New York.

199 Toteu, S.F., Michard, A., Bertrand, J.M., Rocci, G., 1987. U/Pb dating of Precambrian  
200 rocks from northern Cameroon, orogenic evolution and chronology of the Pan-  
201 African belt of central Africa. *Precamb. Res.* 37, 71–87.

202 Toteu, S.F., Penaye, J., Djomani, Y.P., 2004. Geodynamic evolution of the Pan-African  
203 belt in central Africa with special reference to Cameroon. *Canadian Journal of*  
204 *Earth Sciences* 41, 73–85.

205 Valeton, I., 1991. Bauxites and associated terrestrial sediments in Nigeria and their  
206 position in the bauxite belts of Africa. *Journal of African Earth Sciences (and the*  
207 *Middle East)* 12, 297–310.

208 Vasconcelos, P.M., Heim, J.A., Farley, K.A., Monteiro, H., Waltenberg, K. 2013.  
209  $^{40}\text{Ar}/^{39}\text{Ar}$  and (U-Th)/He –  $^4\text{He}/^3\text{He}$  geochronology of landscape evolution and  
210 channel iron deposit genesis at Lynn Peak, Western Australia. *Geochim.*  
211 *Cosmochim. Acta* 117, 283-312.

212 Widdowson, M. 1997. Tertiary palaeosurfaces of the SW Deccan, Western India:  
213 implications for passive margin uplift. In: Widdowson, M. (ed.) *Palaeosurfaces:*  
214 *Recognition, Reconstruction and Palaeoenvironmental Interpretation.* Geological  
215 Society, London, Special Publications, 120, 221–248.

216  
217  
218  
219  
220  
221  
222

223 **FIGURE CAPTIONS**

224 Figure 1. (a) Simplified geologic map of Cameroon showing main domains of the  
225 Neoproterozoic Pan-African orogenic belt. CCSZ: Central Cameroon Shear Zone; (b)  
226 Morpho-geological map across Adamaoua highland (see frame in figure 1a). (b) River  
227 long profiles of Djerem and its tributaries punctuated by knickzones (black and grey  
228 dots for knickzones on Djerem and tributaries, respectively). Geological maps adapted  
229 from Toteu et al. (2004); see frame in Figure 1b for colored segments on x axis in Fig.  
230 1c.

231 Figure 2. (a) Spatial coverage of lateritic landsurfaces and their erosional terrains in  
232 southern Adamaoua highland (Frame in Fig. 1b). (b) Detailed River long profiles of  
233 sections of Djerem and its tributaries that are punctuated by knickzones (black dots for  
234 Djerem and grey dots for tributaries). Colored horizontal bands represent altitudes range  
235 of each landsurface. Colored segments on x axis of (c) represent different lithologies.  
236 (Frame in Fig. 1c).

237 Figure 3. a) Landscape of Adamaoua highland with middle and the lower landsurface.  
238 (b) to (d) Topographic sections across successive lateritic landsurfaces of the Adamaoua  
239 highland over granitic basement. See linear traces of L1 to L2 sections on Figures 2a.

240 Figure 4. (a) 3D interpretations of Google Earth images (© 2022 Maxar technologies);  
241 (a) remnants of the upper and middle landsurfaces; (b) remnants of the middle and  
242 lower landsurfaces. Vertical exaggeration x3. See frames on Fig. 2a.

243 Figure 5. (a) Lateritic regolith of gently sloped upper landsurface; (b) lateritic profile  
244 section in the upper landsurface showing a thick mottled clay beneath the ferricrete.  
245 (Location: N 06°54'54,9", E 013°07'53,4", 1155 m a.s.l); (c) Gentle slope of middle  
246 landsurface exposing iron duricrust (yellow dashed line) and mottled clays. (d) Scarped



247 slope limiting the middle landsurface exposing disaggregated blocs of iron duricrust; (e)  
248 Duricrusted lateritic Regolith on gently sloping lower landsurface; (f) Shallow incision  
249 upslope lower landsurface.

250 Figure 6. Petrographic structure of lateritic regolith of the upper landsurface. (a)  
251 Nodular ferricrete; (b) Duricrusted lateritic relic (yellow dashed line) encompassed in  
252 the nodular iron duricrust. Location of a and b: N 6°59'45.63", E 13°7'49.40", 1194 m  
253 a.s.l.; (c) Paranodular petrographic structure of ferricrete encompassed in nodular  
254 ferricrete; (d) Massive red ferruginous bauxite shown in Fig. 6b; (e) Nodular yellow-  
255 grey bauxite. Location of b and d: N 7°1'26.87", 13°8'28.09"E, 1199 m a.s.l.; (f)  
256 Yellow-pink bauxite relic with preserved granite texture; (Location of e: N 6°59'21.46",  
257 E 13°8'51.39", 1154 m a.s.l. (Geochemical analyses of 6a, 6d and 6f are given in Fig. 7)

258 Figure 7. Composition diagram ( $\text{SiO}_2\text{-Al}_2\text{O}_3\text{-Fe}_2\text{O}_3$ ) for parent rocks and lateritic  
259 duricrusts sampled in regolith of the three landsurfaces, including the vertical IOL  
260 values scale (see Babechuck, 2014). (See petrographic structures of analyzed lateritic  
261 duricrusts in figures 6, 10 and 11; 1= see Fig. 6a; 2= see Fig. 6d; 3= see Fig. 6f; 4= see  
262 Fig. 10d; 5= see Fig. 10d; 6= see Fig. 11a; 7= see Fig. 11b; 8= see Fig. 11c).

263 Figure 8. Trace elements compositions of lateritic duricrusts in regolith of each  
264 landsurface normalized to respective granitoid.

265 Figure 9. REE compositions of lateritic duricrusts in regolith of each landsurface  
266 normalized to respective granitoid.

267 Figure 10. Petrographic structure of lateritic regolith of the middle landsurface. (a)  
268 Nodular structure of ferricrete; (b) Detrital duricrusted lateritic relic (yellow dashed  
269 line) encompassed in the nodular ferricrete; (c) Detailed structure of duricrusted lateritic  
270 relic shown in (b); (d) Purple-reddish nodular ferricrete relic; (Location: N 7°5'47.05",

271 E 13°11'57.32", 1077 m a.s.l. (Geochemical compositions of 10a and 10c are given in  
272 Fig. 7).

273 Figure 11. Petrographic structures of lateritic regolith covering the lower landsurface.  
274 (a) Saprolitic weathered granitoid; (b) duricrusted mottled clays, (c) ferruginous  
275 duricrust with mottled clays relics; (d) Paramodular ferruginous duricrust;  
276 (Geochemical compositions of 11a to 11c are given in Fig. 7).

277 Figure 12. Composition diagram (Ti-Cr-V) for parent rocks and lateritic duricrusts  
278 sampled in regolith of the three landsurfaces.

279 Figure 13. Geochemical diagrams of traces vs major oxides for parent rocks and lateritic  
280 duricrusts sampled in regolith of the three landsurfaces. (a) Nb vs  $\text{Al}_2\text{O}_3$ ; (b) Ta vs  
281  $\text{Al}_2\text{O}_3$ ; (c) V vs  $\text{Fe}_2\text{O}_3$ ; (d) Ga vs  $\text{Fe}_2\text{O}_3$ ; (e) Zr vs. Ti; (f) IOL vs. Zr/Ti. (Stoichiometric  
282 linear relation to granites in Fig. 13c is marked by the straight line).

283 Figure 14. Geochemical diagrams of (a) Nb/Y vs Zr/Ti, and REE fractionation in parent  
284 rocks and lateritic duricrusts sampled in regolith of the three landsurfaces. (b)  $\text{Eu}/\text{Eu}^*$   
285 vs Nb/Y; (c)  $(\text{Gd}/\text{Yb})_N$  vs Zr/Ti; (d) HREE vs Th/Y.

286

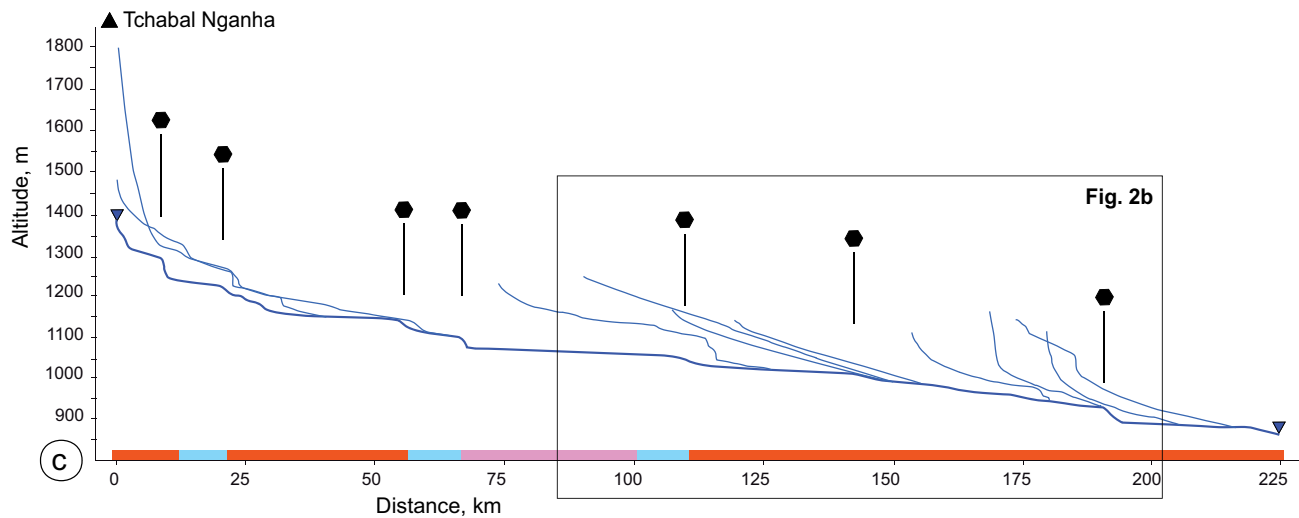
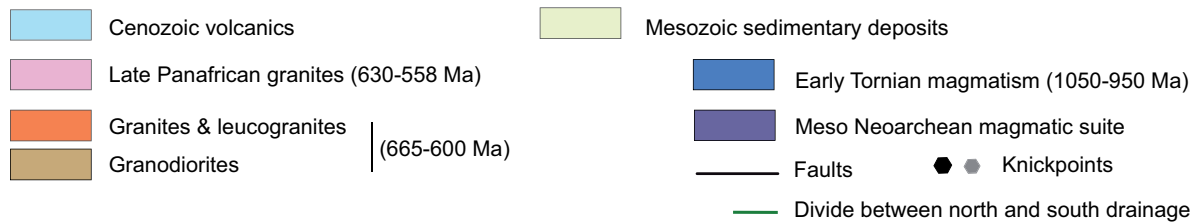
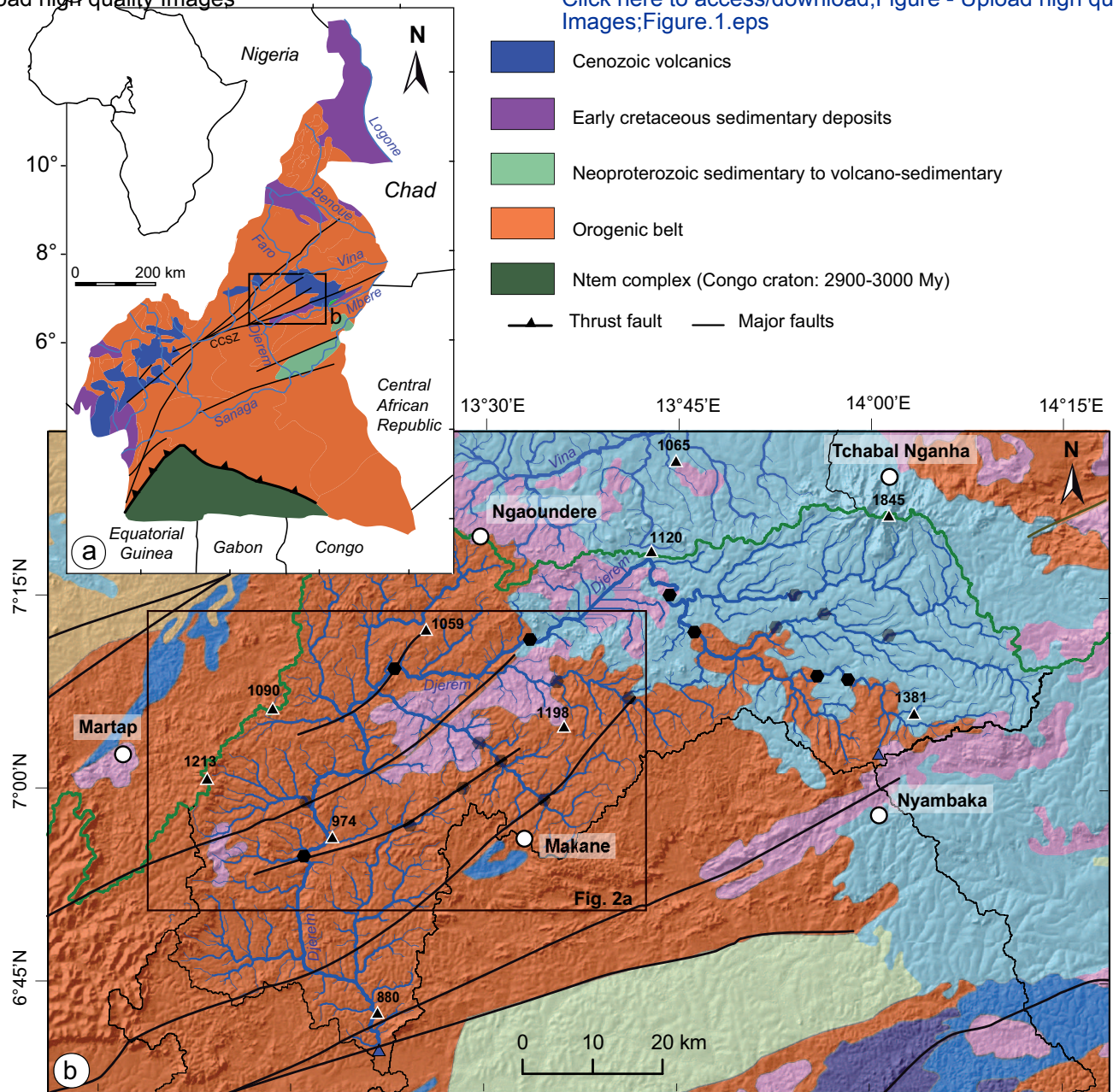


Fig. 1



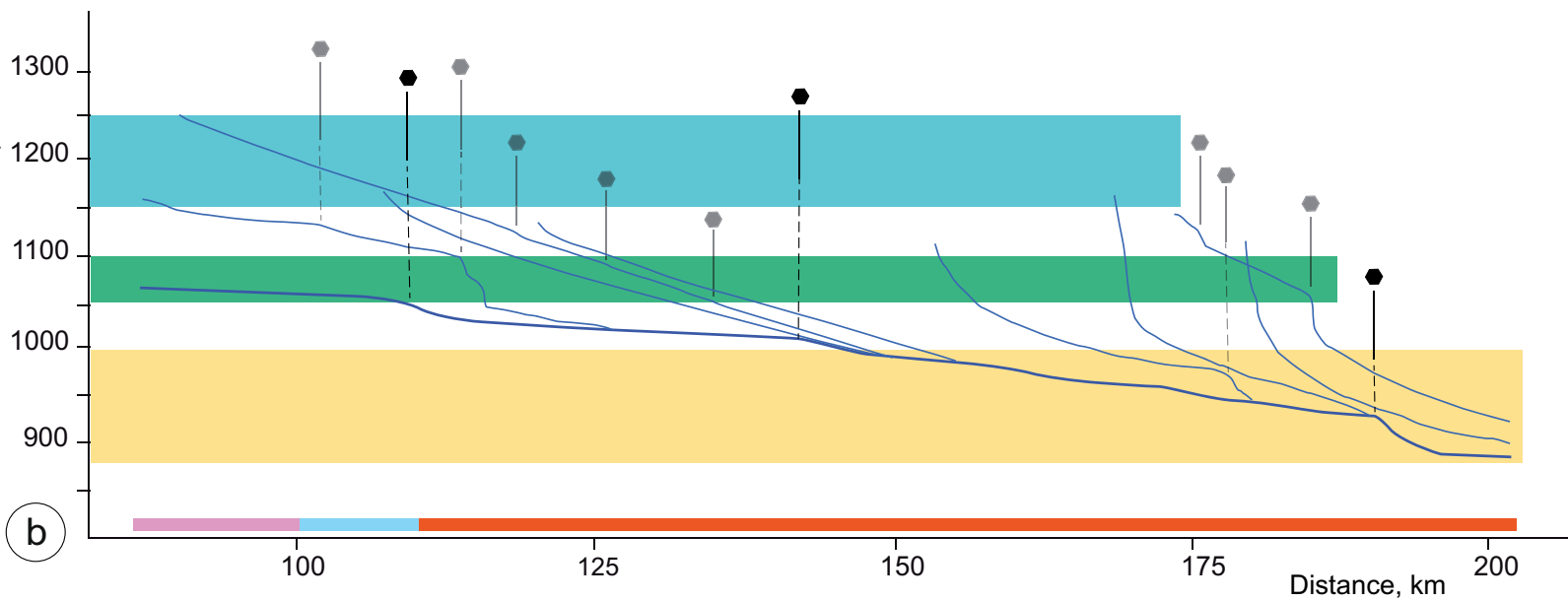
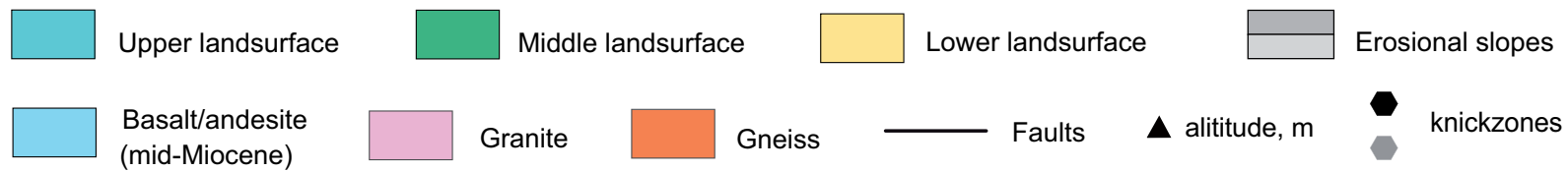
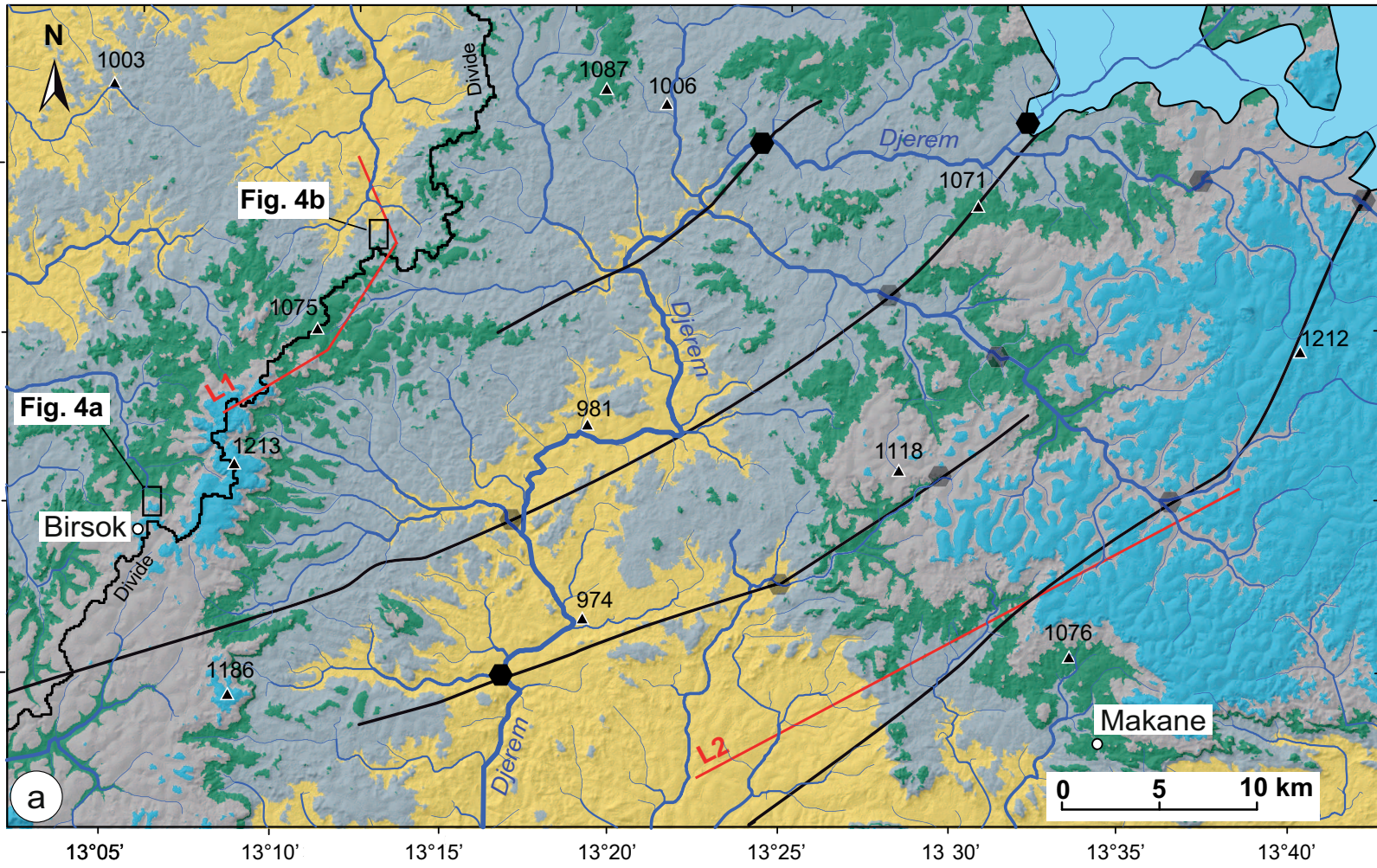


Fig. 2

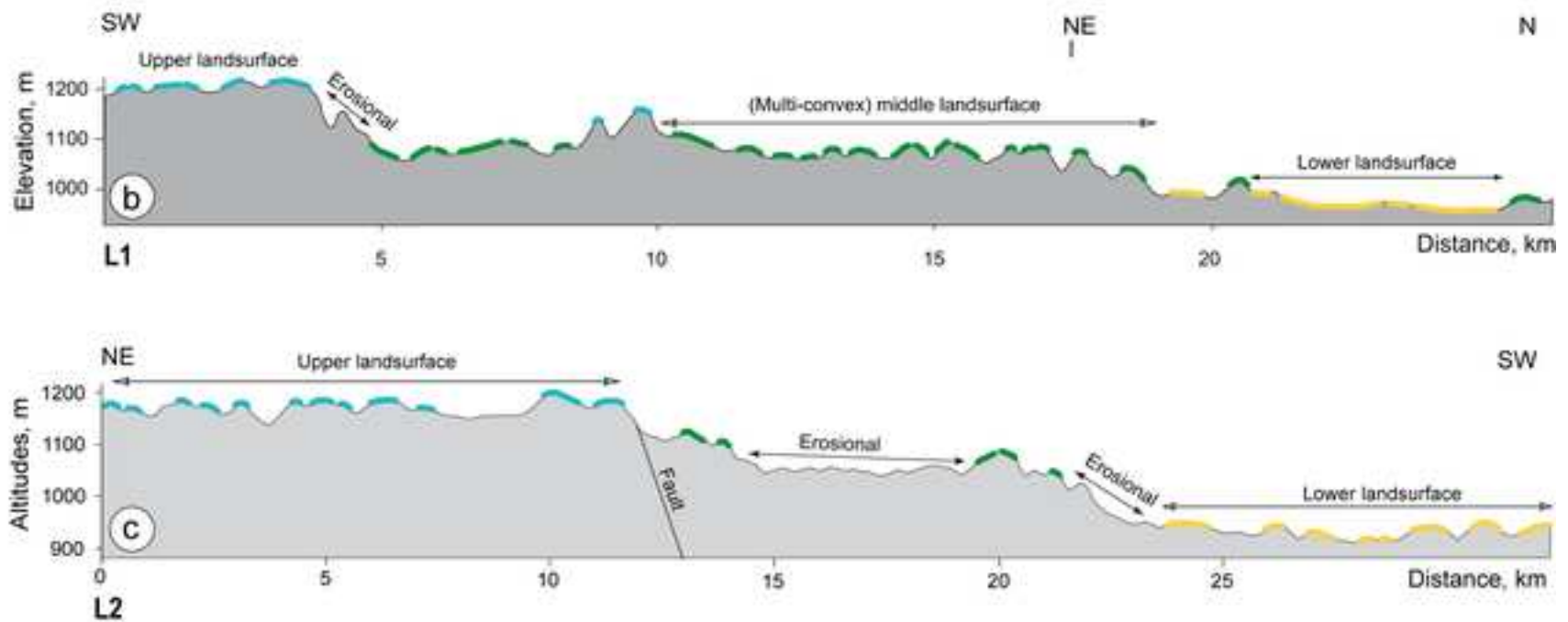
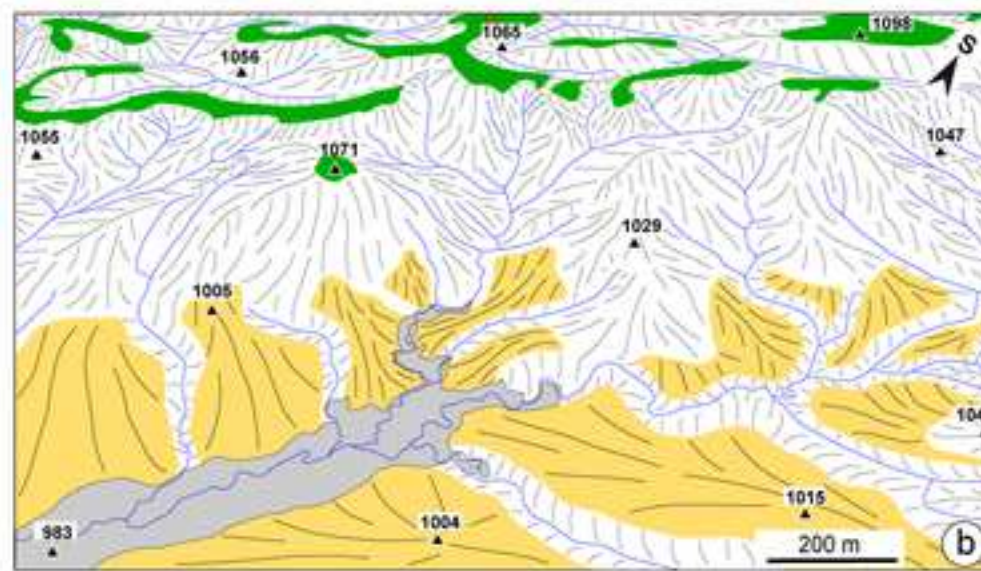
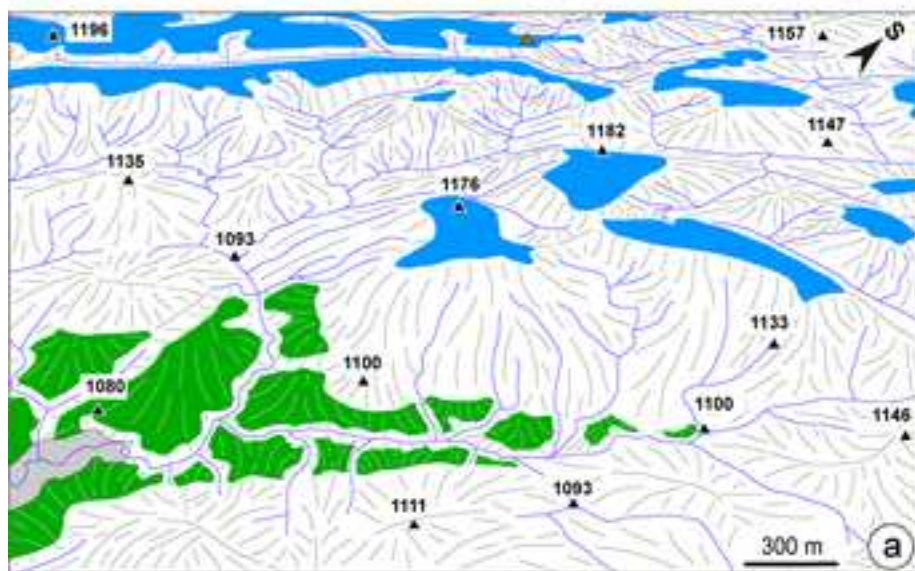


Fig. 3





▲ Latitude : 6.970954° N ; Longitude : 13.126412° E ; Altitude : 1176 m

▲ latitude : 7.09151784°N ; longitude : 13.20427615°E ; altitude: 1086 m

Upper landsurface    
  Erosional slopes    
  Middle landsurface    
  Lower landsurface    
  Alluvial plain    
 ▲ Altitudes, m

Fig. 4





Fig. 5



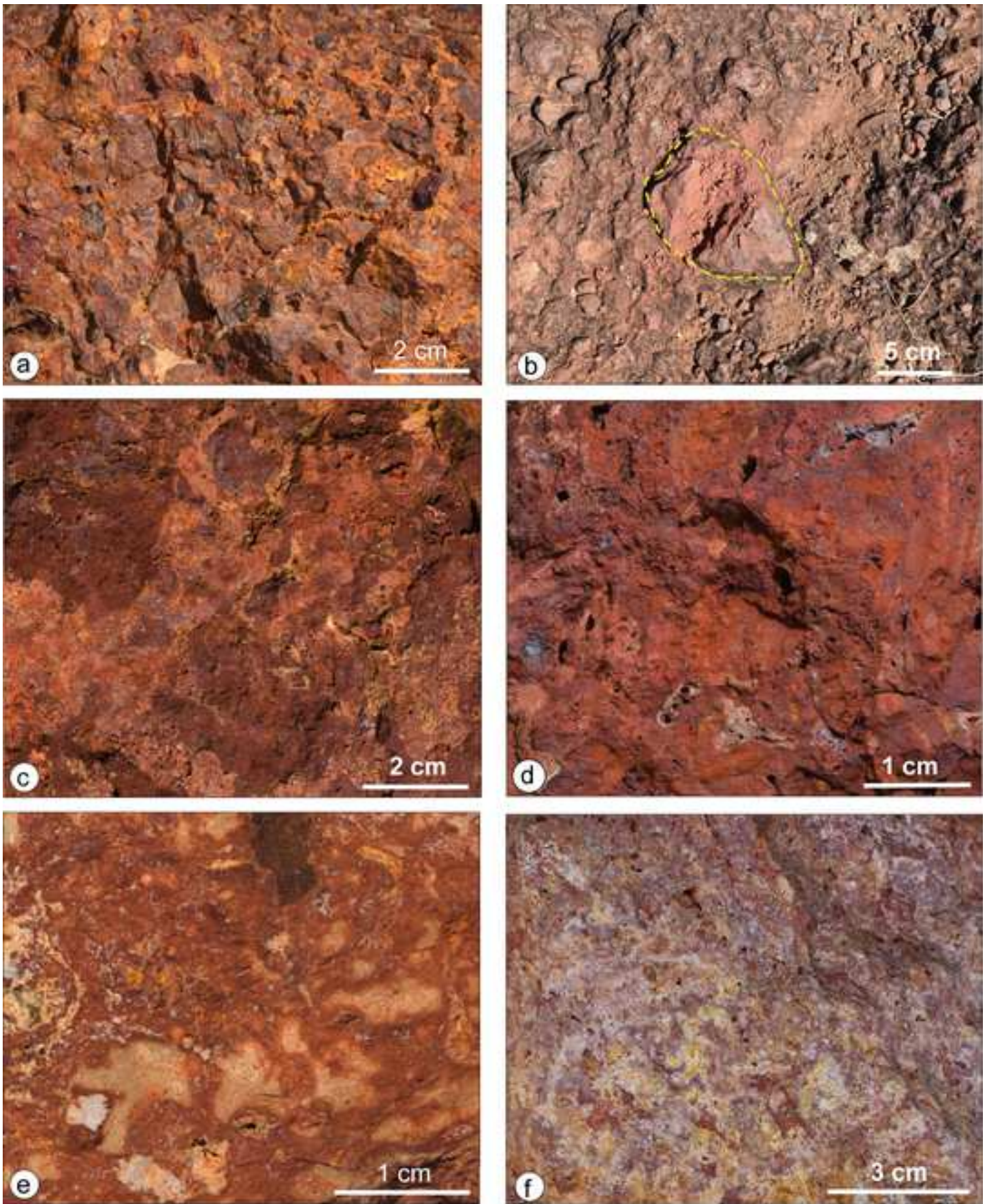


Fig. 6



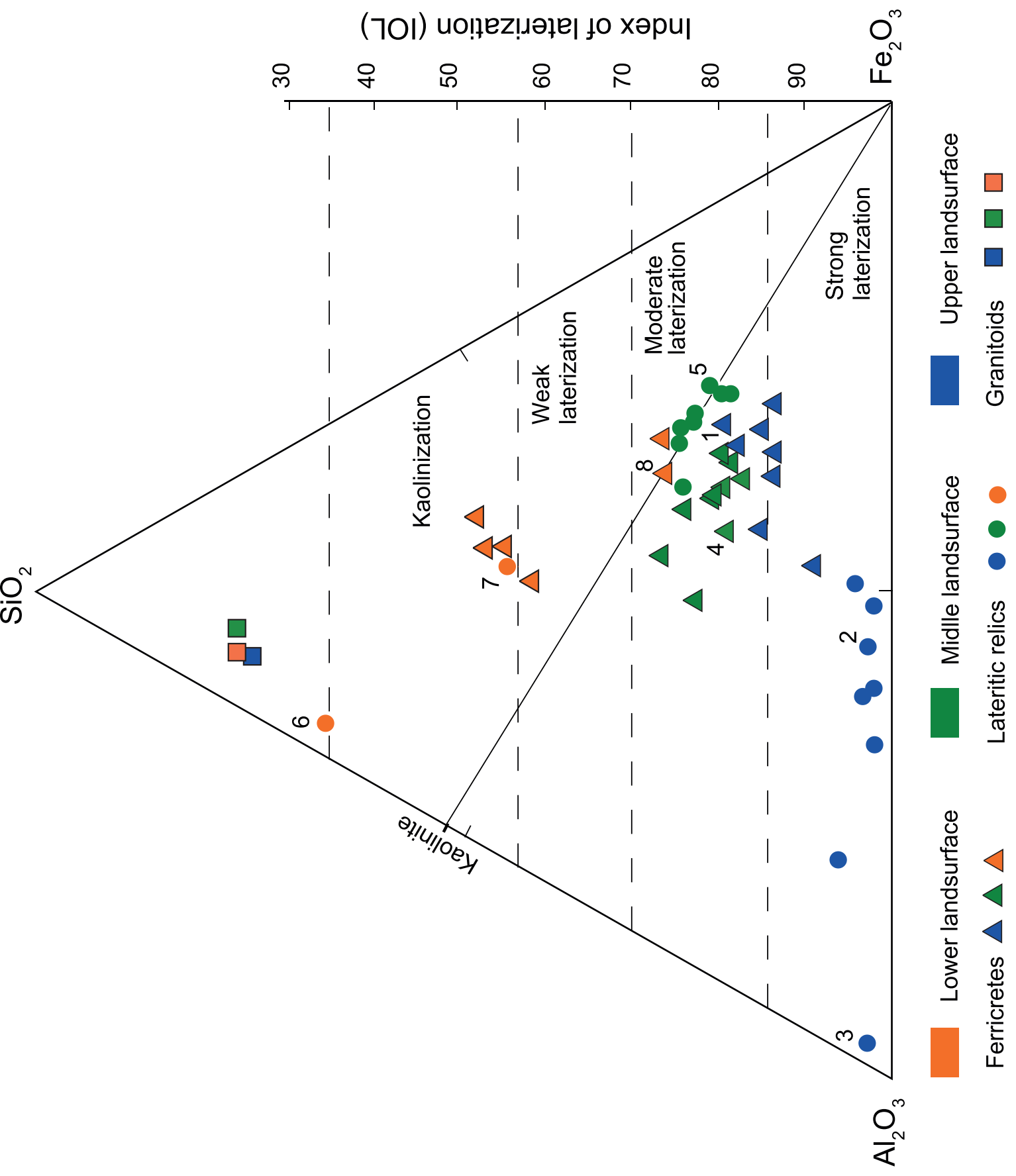


Fig. 7

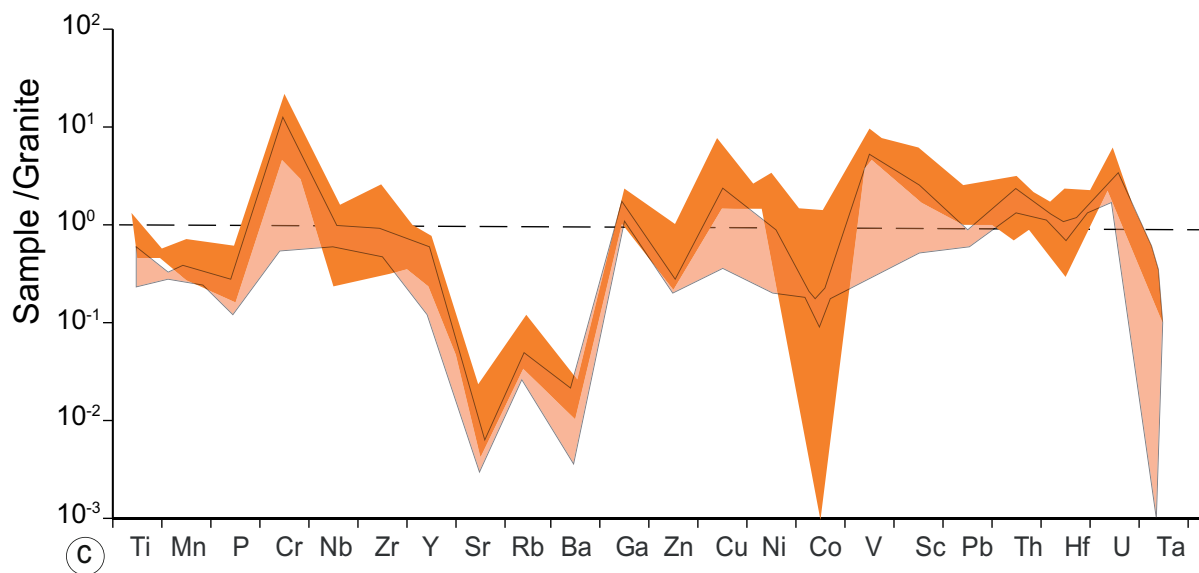
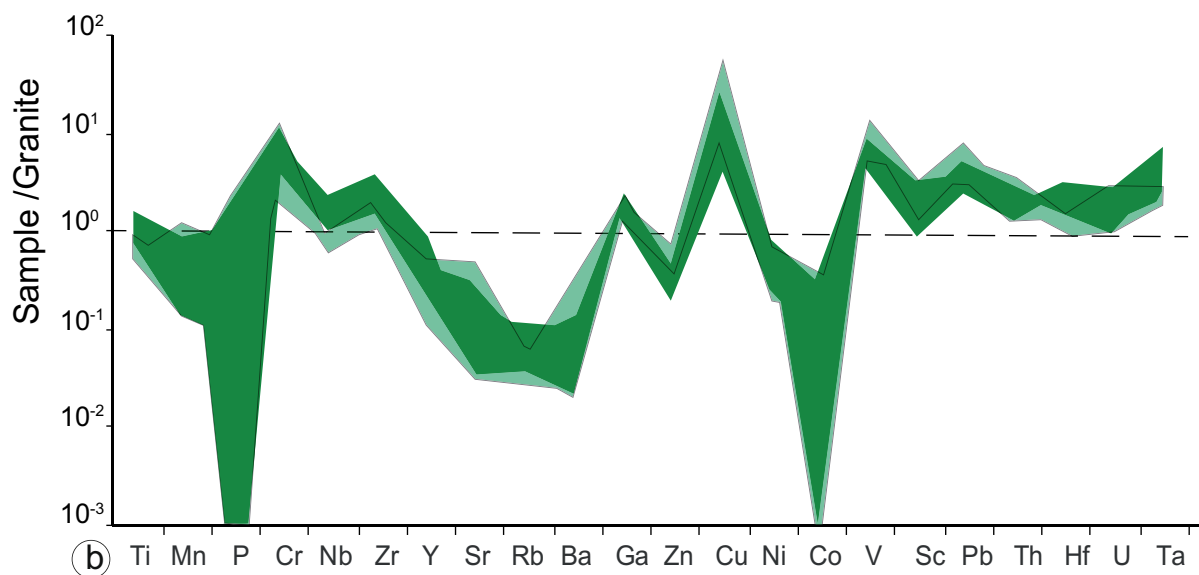
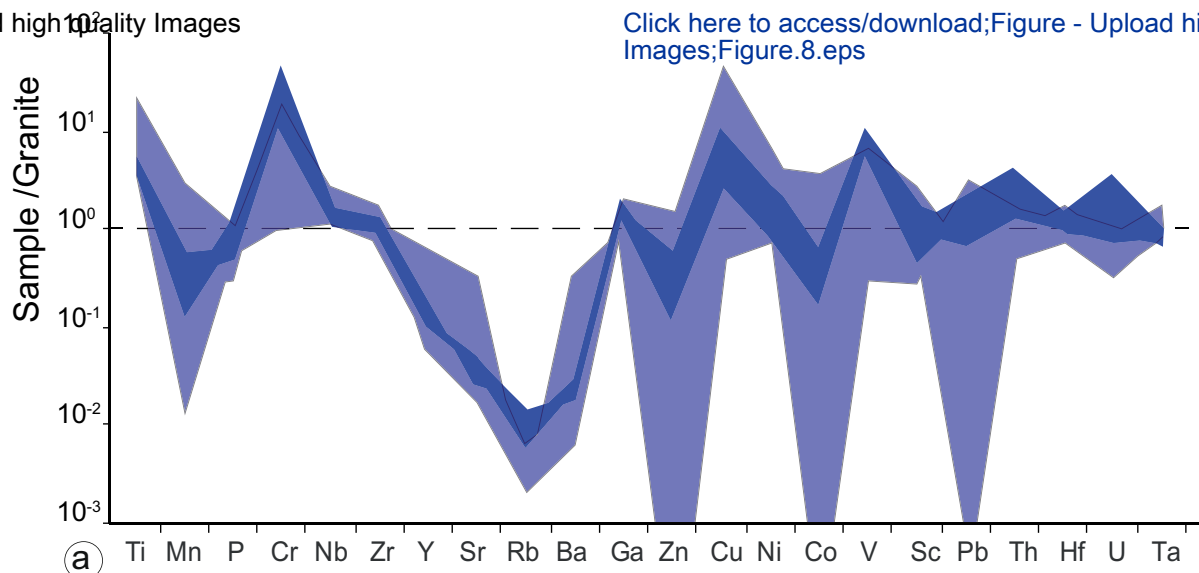


Fig. 8

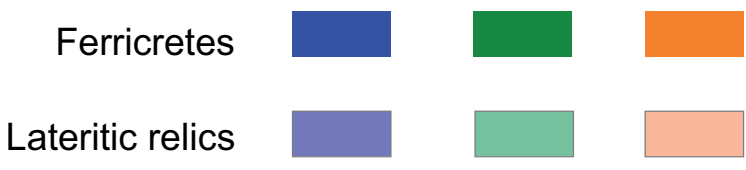
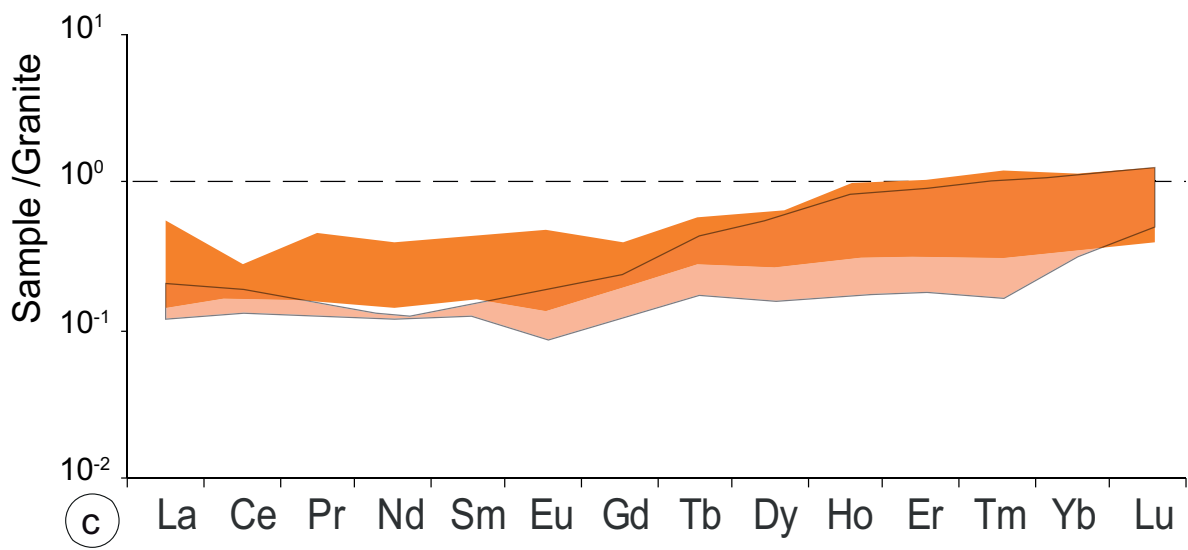
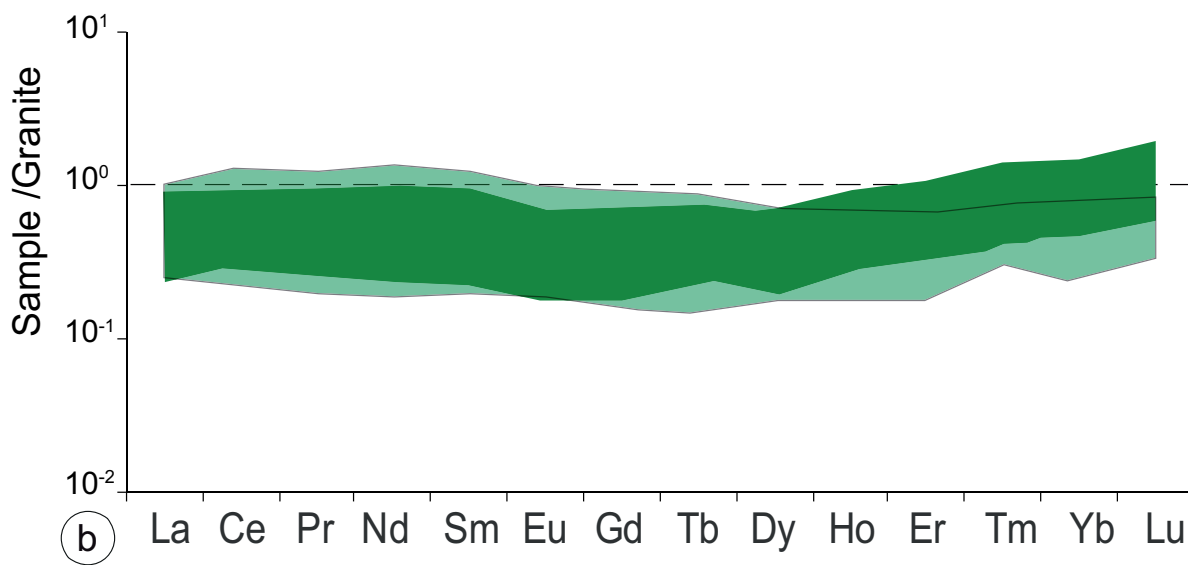
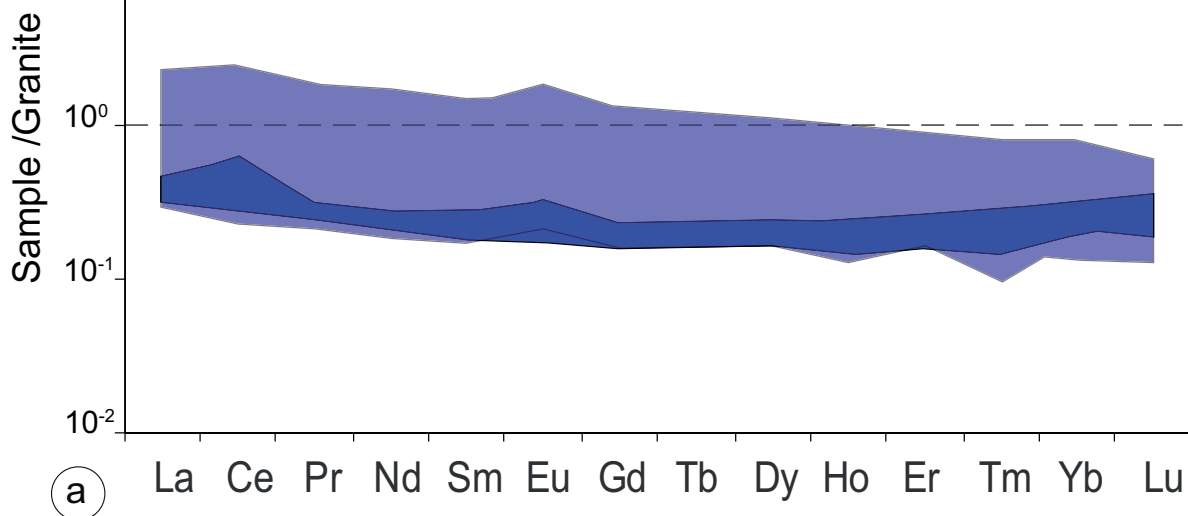


Fig. 9

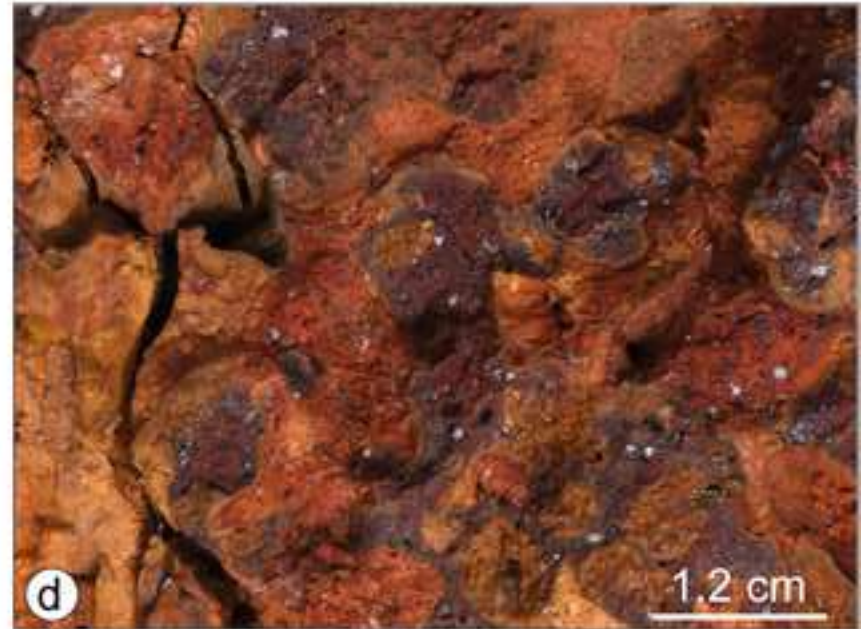
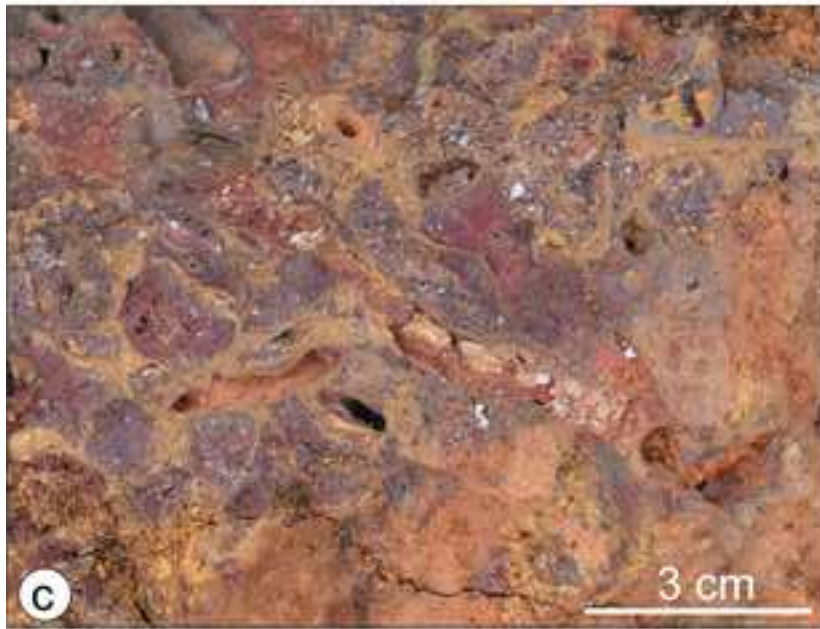
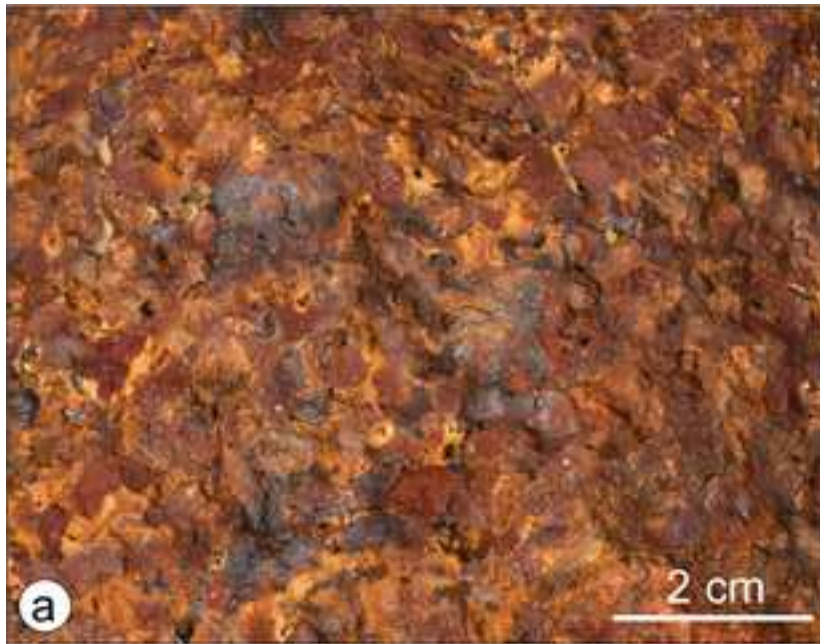


Fig. 10



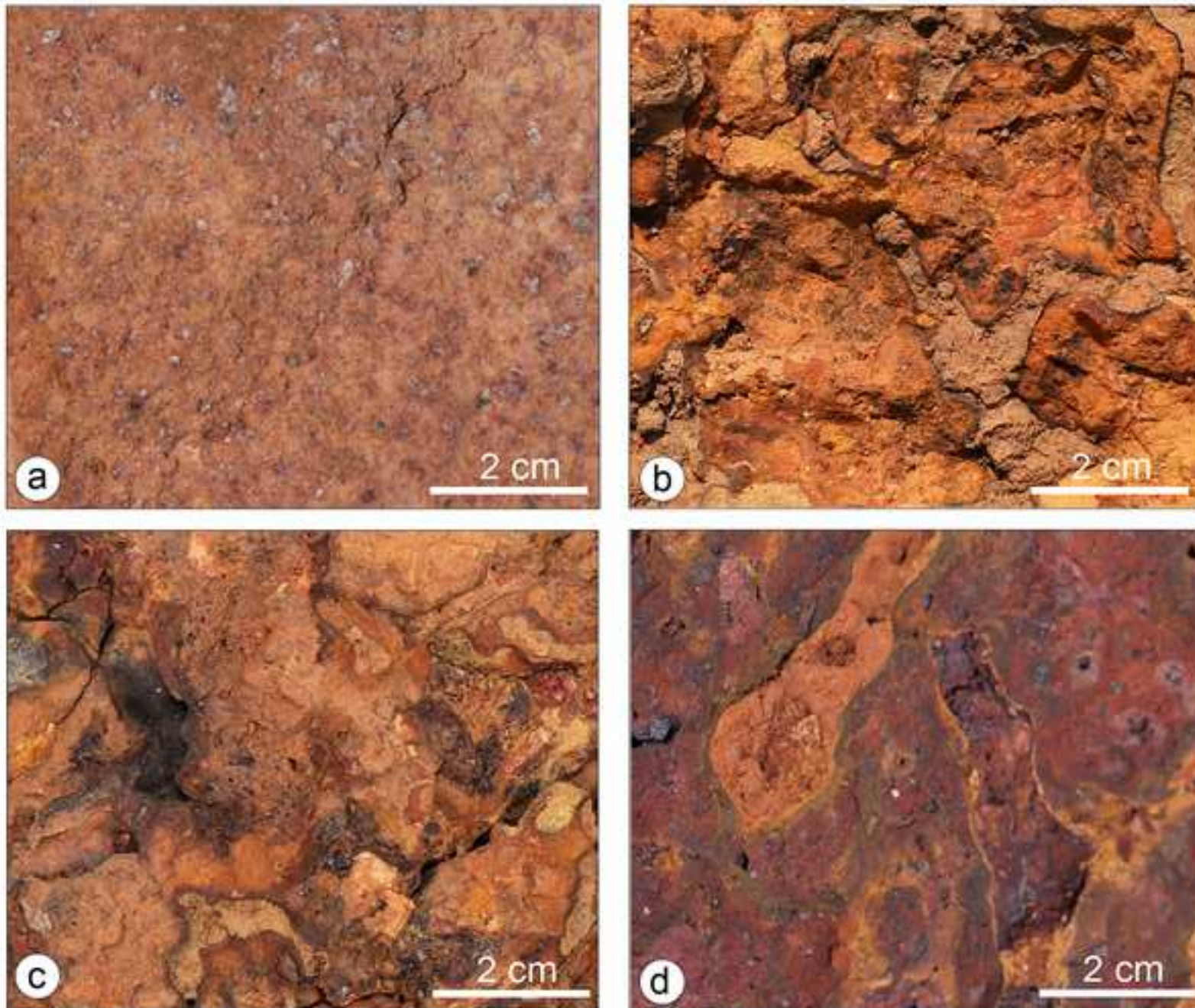


Fig. 11

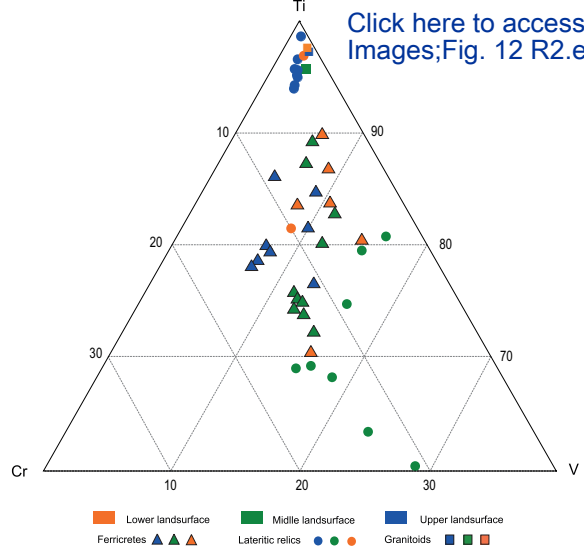


Fig. 12

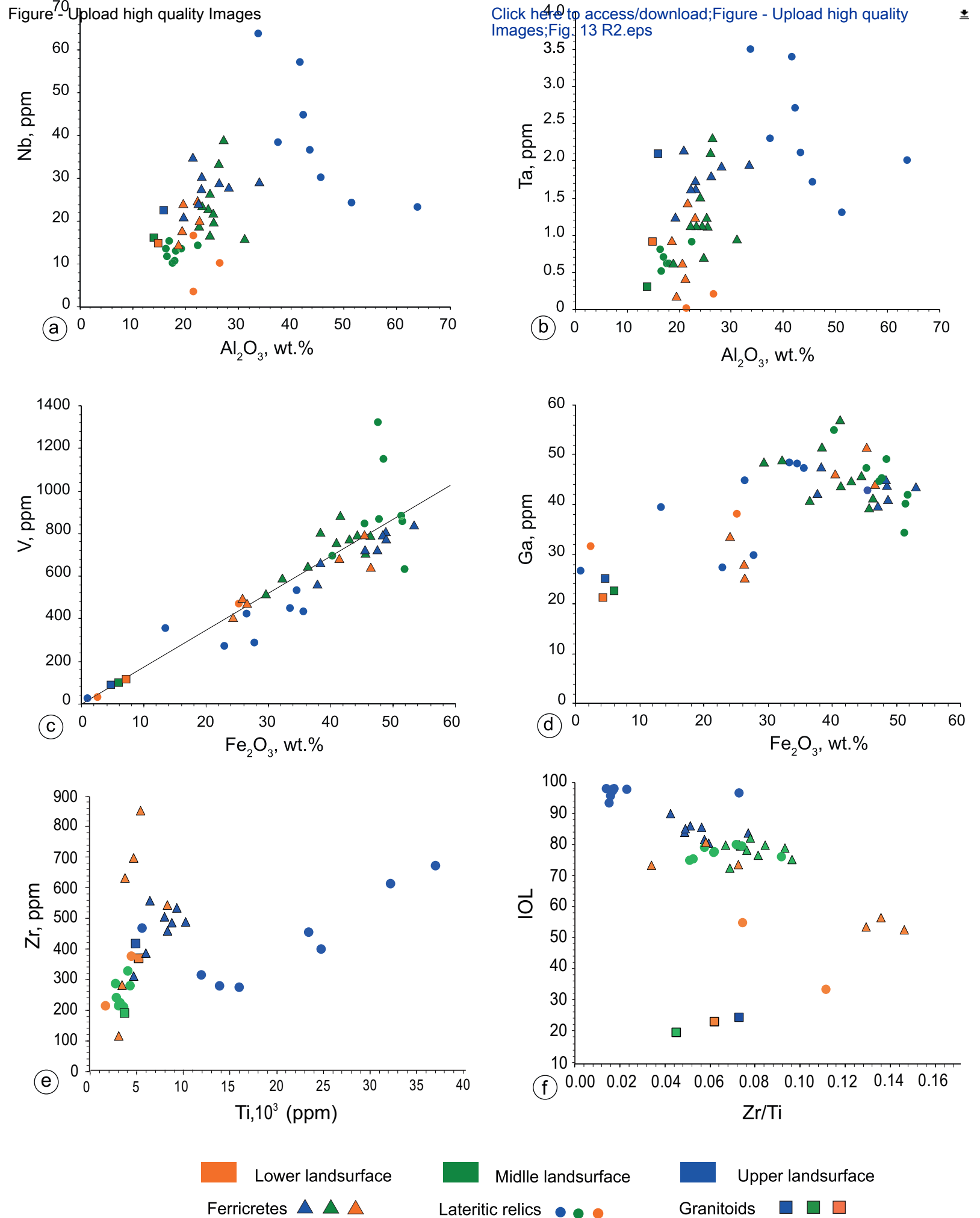


Fig. 13

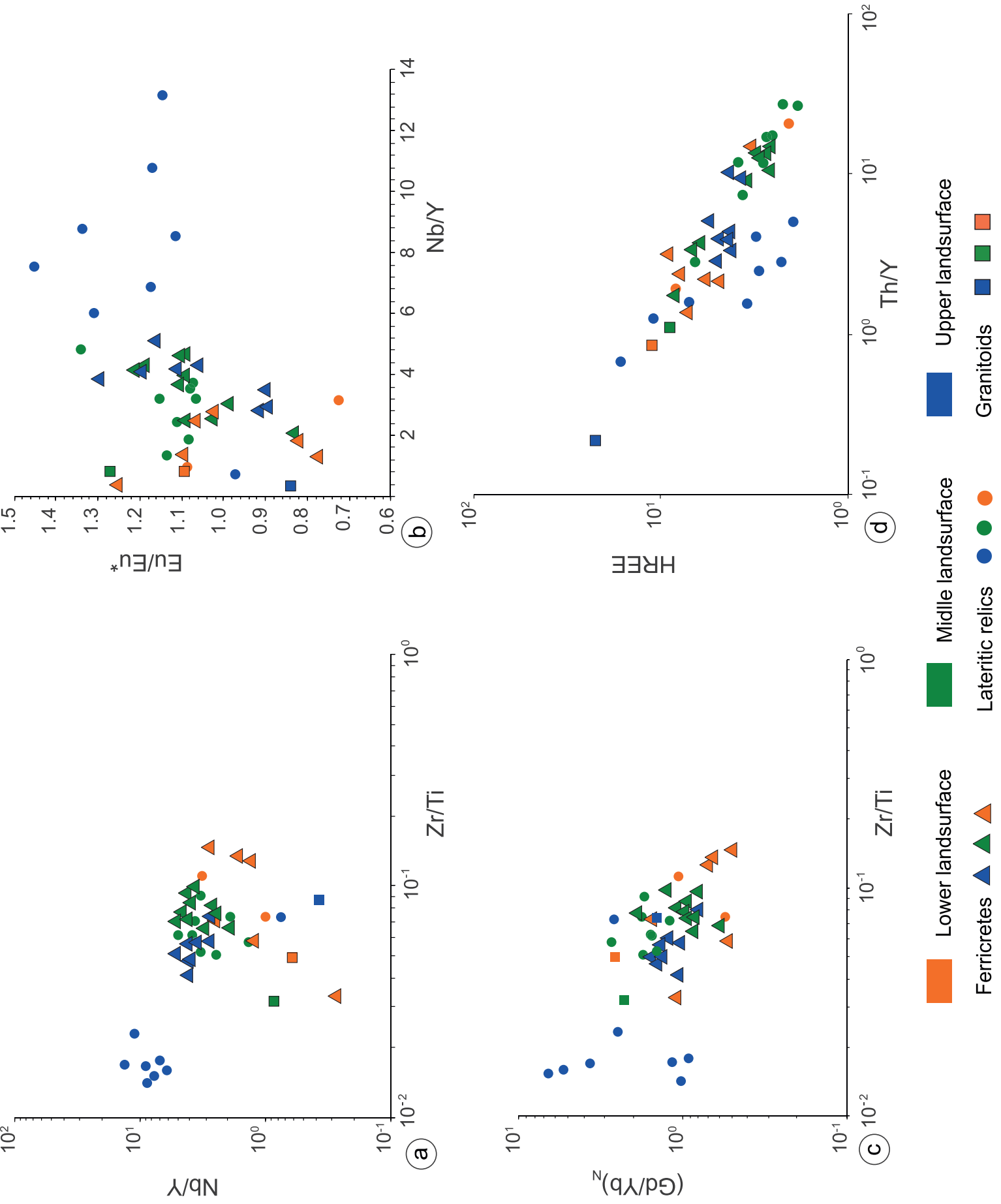


Fig. 14



Supplementary material for “**Lateritic landsurface-regolith differentiation on Pan-African granitic basement of Adamaoua highland, Cameroon**”

Submitted to Catena, July, 13, 2023 by Momo et al., 2023

Samples collected in surface regolith of lateritic landsurfaces were crushed and sieved to ~ 64 mm for geochemical analyses. Major oxides in wt.% and trace + rare earth elements (REE) in ppm were analyzed by ICP-AES (Inductively coupled plasma-atomic emission spectrometry) and ICP-MS (Inductively coupled plasma-Mass spectrometry) (combination of ME-MS81TM + whole rock package ME-ICP-06; www.alsglobal.com) at the ALS Laboratory Group SL (Spain). The main results are reported in the Table DR.

Table DR. Geochemical analyses of lateritic duricrusted regolith and granitic parent rocks for each landsurfaces. (a) Major oxides; (b) Trace elements in ppm; (c) Rare Earth elements in ppm.  $Ce/Ce^* = (Ce_{sample}/Ce_{UCC})/(La_{sample}/La_{UCC})^{1/2} (Pr_{sample}/Pr_{UCC})^{1/2}$ ;  $Eu/Eu^* = (Eu_{sample}/Eu_{UCC})/(Sm_{sample}/Sm_{UCC})^{1/2} (Gd_{sample}/Gd_{UCC})^{1/2}$ ;  $(Gd/Yb)_N = (Gd_{sample}/Gd_{UCC})/(Yb_{sample}/Yb_{UCC})$

DRA. Major oxides in wt.%

Regolith type	Sample	SiO <sub>2</sub>	Al <sub>2</sub> O <sub>3</sub>	Fe <sub>2</sub> O <sub>3</sub>	TiO <sub>2</sub>	CaO	MgO	Na <sub>2</sub> O	K <sub>2</sub> O	MnO	P <sub>2</sub> O <sub>5</sub>	LOI	IOL
Upper landsurface ferricretes	SL-2	13.4	23.10	48.90	1.41	0.03	0.04	0.01	0.03	0.02	0.34	13.4	84.3
	SL-3	11.75	26.40	45.60	1.35	0.02	0.03	0.01	0.02	0.03	0.19	15.05	86.00
	SL-4	7.66	34.10	38.00	1.73	0.01	0.03	0.01	0.01	0.04	0.18	19.05	90.40
	SL-5	11.70	21.20	53.10	1.57	0.01	0.04	0.01	0.03	0.03	0.26	12.75	86.40
	BIR-01	16.10	19.60	48.40	0.79	0.02	0.03	0.01	0.04	0.02	0.38	14.4	80.90
	BIR-02	15.25	22.50	47.20	1.01	0.02	0.03	0.01	0.03	0.02	0.3	13.7	82.00
	M-11	12.20	23.20	48.30	1.48	0.02	0.04	0.01	0.03	0.04	0.24	14	85.40
	MAN-10-1	12.50	28.00	38.30	1.09	0.01	0.02	0.01	0.06	0.01	0.33	18.85	84.10
Upper landsurface relics	SL-A	4.48	51.40	13.45	2.68	0.02	0.03	0.01	0.01	0.01	0.14	27.20	93.50
	SL-B	1.67	41.80	26.50	5.40	0.03	0.18	-	-	0.06	0.29	23.80	97.60
	SL-C	1.30	45.70	23.00	2.34	0.02	0.04	0.01	0.01	0.02	0.18	26.20	98.10
	SL-D	1.48	43.50	27.80	2.01	0.02	0.04	0.01	-	0.03	0.17	24.00	98.00
	SL-E	2.96	33.80	34.60	6.21	0.02	0.15	0.01	0.01	0.22	0.28	20.40	95.90
	BIR-A	1.40	37.60	35.60	4.15	0.03	0.06	0.01	-	0.06	0.10	21.30	98.10
	BIR-C	1.55	42.40	33.40	3.94	0.01	0.05	0.01	-	0.04	0.09	19.05	98.00
	BIR-E	2.16	64.00	0.92	0.96	0.02	0.01	0.01	-	-	0.16	31.90	96.80
Upper landsurface granite	R-BIR-02	63.2	16	4.72	0.85	3.10	1.94	4.13	4.57	0.08	0.33	0.79	99.98
Middle landsurface ferricretes	KAL-1	17.25	22.30	46.00	0.74	0.04	0.05	0.01	0.03	0.02	0.27	13.85	79.80
	KAL-2	16.75	23.10	45.70	0.79	0.07	0.07	0.01	0.05	0.02	0.21	12.30	80.40
	KAL-3	17.55	25.30	41.40	0.77	0.03	0.03	-	0.06	0.02	0.17	15.35	79.20
	KAL-4	17.00	25.50	43.00	0.78	0.02	0.03	0.01	0.04	0.02	0.13	15.15	80.10
	KAL-5	14.55	24.40	44.30	0.82	0.03	0.02	0.01	0.04	0.02	0.14	15.5	82.50
	LO-1	15.70	26.7	36.70	1.43	0.02	0.05	0.02	0.06	0.06	0.46	18.25	80.20
	KAL-01	20.20	24.50	38.40	0.66	0.02	0.03	-	0.05	0.02	0.25	15.65	75.70
	LIK-08-1	21.80	26.00	32.20	1.41	0.01	0.05	0.01	0.12	0.02	0.11	17.8	72.80
	MAN-02	17.75	24.10	41.10	1.04	-	0.02	-	0.08	0.01	0.32	16.35	78.60
	MAN-04	18.05	30.70	29.60	0.64	-	0.02	0.01	0.07	0.02	0.22	19	77.00
Middle landsurface relics	MAN-03-a	20.70	22.40	40.30	0.62	-	0.02	-	0.05	0.01	0.26	14.95	75.20
	KAL-A	16.90	17.10	51.40	0.69	0.08	0.07	0.01	0.03	0.04	0.23	12.5	80.20
	KAL-C	20.90	19.30	45.50	0.61	0.03	0.03	-	0.05	0.01	0.18	13.45	75.60
	KAL-D	17.35	16.55	51.80	0.49	0.06	0.07	0.01	0.02	0.09	0.28	13.9	79.80
	KAL-E	18.90	18.15	47.80	0.55	0.04	0.03	0.01	0.06	0.01	0.19	13.2	77.70

	LO-B	17.60	16.45	51.50	0.73	0.02	0.02	0.01	0.04	0.01	0.57	12.95	79.40
	KAL-I	18.85	18.05	48.50	0.52	0.04	0.03	0.02	0.05	0.02	0.17	12.75	77.90
	KAL-J	20.20	17.70	47.60	0.47	0.01	0.02	0.04	0.03	0.01	0.19	12.8	76.40
Middle landsurface granite	R-KAL	64.3	14	6.04	0.63	4.68	2.33	3.63	2.17	0.07	0.25	0.80	99.05
Lower landsurface ferricretes	HG-01	41.1	19.8	26.50	0.65	0.03	0.08	0.02	0.17	0.02	0.21	12.10	53.00
	DIR-01	15.85	22.1	45.40	1.40	0.01	0.03	-	0.1	0.02	0.12	15.25	81.00
	TEK-03	23	18.7	46.60	0.59	0.02	0.03	0.03	0.07	0.03	0.15	12.25	74.00
	LIK-01	35.7	22.9	24.40	0.94	0.02	0.08	0.01	0.16	0.02	0.07	14.85	57.00
	LIK-05	38.7	19.45	26.10	0.81	-	0.06	0.01	0.13	0.02	0.19	13.85	54.10
	LIK-07	22.1	21.5	40.60	0.52	-	0.03	-	0.07	0.05	0.22	14.10	73.80
Lower landsurface relics	TEK-05-a	56.6	26.6	2.53	0.29	-	0.01	0.01	0.06	0.03	0.06	14.00	34.00
	LIK-8-a	38	21.5	25.20	0.76	-	0.03	0.02	0.19	0.02	0.11	14.00	55.10
Lower landsurface granite	R-LO	63.2	14.95	4.44	0.89	3.64	1.86	3.91	4.54	0.07	0.42	1.03	99.39

## DRb. Trace elements

Regolith type	Sample	Cr	Nb	Zr	Y	Sr	Rb	Ba	Zn	Cu	Ni	Co	V	Sc	Pb	Th	Hf	U	Ta	Nb/Y	Zr/Ti	Th/Y
Upper landsurface ferricretes	SL-2	1360.00	27.70	413.00	6.80	40.50	2.20	56.30	34.00	30.00	35.00	6.00	799.00	10.00	29.00	19.80	9.60	4.08	1.70	4.07	0,05	2.91
	SL-3	1440.00	28.50	455.00	6.80	32.20	2.10	50.90	33.00	28.00	40.00	6.00	714.00	4.00	31.00	23.90	10.60	4.24	1.80	4.19	0,06	3.51
	SL-4	1080.00	29.10	441.00	7.10	28.70	1.30	42.40	43.00	36.00	43.00	4.00	556.00	8.00	17.00	17.80	10.20	5.61	1.90	4.10	0,04	2.51
	SL-5	1510.00	35.00	482.00	6.90	38.60	1.80	52.00	34.00	30.00	33.00	6.00	827.00	12.00	28.00	23.10	11.10	3.18	2.10	5.07	0,05	3.35
	BIR-01	650.00	21.00	281.00	6.90	29.60	3.80	44.00	26.00	18.00	17.00	2.00	769.00	15.00	30.00	58.50	7.30	8.39	1.20	3.04	0,06	8.48
	BIR-02	650.00	23.40	348.00	6.60	32.20	2.80	35.20	16.00	16.00	15.00	2.00	711.00	10.00	46.00	50.30	9.40	6.06	1.60	3.55	0,06	7.62
	M-11	1680.00	30.10	437.00	7.10	43.00	1.80	56.90	29.00	25.00	33.00	3.00	775.00	8.00	38.00	23.70	10.60	4.29	1.60	4.24	0,05	3.34
	MAN-10-1	511.00	27.80	503.00	10.00	23.40	3.00	33.20	11.00	13.00	14.00	2.00	650.00	9.00	30.00	41.80	12.15	14.30	1.90	2.78	0,08	4.18
Upper landsurface relics	SL-A	600.00	24.20	247.00	3.20	44.30	0.60	19.40	101.00	65.00	30.00	11.00	353.00	5.00	8.00	11.15	6.60	2.09	1.30	7.56	0,02	3.48
	SL-B	660.00	57.20	548.00	6.50	61.80	1.10	46.90	118.00	34.00	47.00	14.00	419.00	18.00	3.00	9.15	14.40	3.74	3.40	8.80	0,02	1.41
	SL-C	380.00	30.30	250.00	4.40	15.30	0.50	16.00	70.00	169.00	90.00	3.00	267.00	11.00	0.00	6.12	6.50	2.34	1.70	6.89	0,02	1.39
	SL-D	460.00	36.70	282.00	3.40	40.80	0.40	30.50	24.00	19.00	16.00	8.00	284.00	7.00	4.00	8.32	7.50	1.41	2.10	10.79	0,02	2.45
	SL-E	570.00	63.90	598.00	10.60	141.50	0.40	80.40	121.00	57.00	58.00	38.00	532.00	22.00	11.00	11.95	15.10	3.08	3.50	6.03	0,02	1.13
	BIR-A	660.00	38.50	356.00	4.50	20.20	0.50	13.50	58.00	33.00	51.00	19.00	432.00	21.00	7.00	9.79	9.30	4.20	2.30	8.56	0,01	2.18
	BIR-C	690.00	44.80	406.00	3.40	13.60	0.40	11.40	58.00	20.00	22.00	9.00	445.00	12.00	7.00	14.25	10.90	3.46	2.70	13.18	0,02	4.19
	BIR-E	40.00	23.30	421.00	32.00	230.00	0.40	519.00	0.00	2.00	10.00	0.00	24.00	2.00	69.00	19.95	10.60	3.36	2.00	0.73	0,07	0.62
Upper landsurface granite	R-BIR-02	40.00	22.40	374.00	60.30	845.00	205.00	1890.00	85.00	4.00	15.00	11.00	84.00	8.00	23.00	13.00	9.50	4.56	2.10	0.37	0.07	0.22
Middle landsurface ferricretes	KAL-1	770.00	18.80	327.00	4.50	12.30	2.40	25.40	24.00	49.00	26.00	0.00	782.00	8.00	53.00	47.60	7.50	4.61	1.10	4.18	0,07	10.58
	KAL-2	800.00	22.90	345.00	4.90	15.70	2.60	29.20	26.00	53.00	25.00	1.00	707.00	9.00	55.00	52.90	8.90	5.14	1.10	4.67	0,07	10.80
	KAL-3	830.00	21.20	431.00	5.00	10.70	3.30	23.60	22.00	47.00	26.00	2.00	739.00	8.00	46.00	53.00	9.90	5.32	1.20	4.24	0,09	10.60
	KAL-4	790.00	19.60	396.00	5.00	10.80	2.90	26.20	19.00	51.00	23.00	2.00	769.00	9.00	42.00	53.30	9.40	4.45	1.10	3.92	0,08	10.66
	KAL-5	830.00	22.40	383.00	4.80	9.90	2.90	21.20	15.00	35.00	19.00	3.00	780.00	11.00	41.00	54.40	9.90	6.12	1.10	4.67	0,08	11.33
	LO-1	580.00	38.70	574.00	12.90	44.20	6.70	85.40	16.00	21.00	17.00	4.00	647.00	9.00	25.00	37.50	15.50	12.15	2.30	3.00	0,07	2.91
	KAL-01	690.00	16.80	382.00	4.60	12.20	6.20	39.20	26.00	25.00	28.00	1.00	802.00	10.00	41.00	39.60	9.20	5.32	0.70	3.65	0,10	8.61
	LIK-08-1	441.00	32.90	581.00	16.30	12.20	7.10	41.30	13.00	30.00	29.00	3.00	576.00	20.00	29.00	25.30	14.40	9.27	2.10	2.02	0,07	1.55
	MAN-02	632.00	26.00	476.00	10.40	83.70	4.70	131.50	24.00	13.00	24.00	1.00	880.00	29.00	38.00	31.90	11.35	11.65	1.50	2.50	0,08	3.07
	MAN-04	282.00	15.45	312.00	5.70	25.60	4.80	40.30	14.00	9.00	9.00	1.00	506.00	11.00	36.00	42.80	7.55	9.73	0.90	2.71	0,08	7.51
Middle landsurface relics	MAN-03-a	255.00	14.35	190.00	5.90	27.80	4.50	37.10	32.00	21.00	23.00	2.00	690.00	20.00	36.00	36.20	4.66	9.80	0.90	2.43	0,05	6.14
	KAL-A	490.00	15.30	297.00	4.30	18.90	3.10	47.40	34.00	71.00	23.00	4.00	879.00	13.00	43.00	40.60	7.40	5.00	0.70	3.56	0,07	9.44
	KAL-C	770.00	13.50	193.00	4.20	8.90	3.20	21.90	25.00	68.00	19.00	0.00	845.00	12.00	59.00	56.30	4.90	5.09	0.60	3.21	0,05	13.40
	KAL-D	670.00	11.70	218.00	6.20	10.60	2.00	27.10	49.00	115.00	24.00	3.00	629.00	27.00	37.00	58.90	5.30	7.40	0.50	1.89	0,07	9.50
	KAL-E	650.00	13.10	204.00	3.50	8.90	4.60	23.20	30.00	73.00	26.00	3.00	867.00	21.00	49.00	48.20	5.30	4.77	0.60	3.74	0,06	13.77

	LO-B	170.00	13.50	253.00	10.10	143.00	3.40	273.00	35.00	21.00	7.00	2.00	855.00	30.00	31.00	24.70	6.60	12.40	0.80	1.34	0,06	2.45
	KAL-I	640.00	10.70	194.00	2.20	8.70	3.40	20.50	25.00	80.00	21.00	3.00	1145.00	31.00	69.00	45.20	4.51	4.59	0.60	4.86	0,06	20.55
	KAL-J	520.00	10.25	259.00	3.20	11.50	2.70	25.20	25.00	69.00	18.00	1.00	1320.00	25.00	55.00	66.90	5.98	5.06	0.60	3.20	0,09	20.91
Middle landsurface granite	R-KAL	70.00	16.20	172.00	19.10	288.00	65.90	977.00	69.00	2.00	35.00	13.00	96.00	9.00	10.00	19.25	4.70	1.71	0.30	0.85	0.05	1.01
Lower landsurface ferricretes	HG-01	280.00	23.60	570.00	8.40	10.90	16.70	30.40	13.00	21.00	27.00	8.00	460.00	12.00	31.00	15.30	14.40	8.55	0.60	2.81	0,15	1.82
	DIR-01	850.00	23.80	489.00	19.10	6.30	4.80	34.90	53.00	107.00	14.00	0.00	784.00	28.00	31.00	52.10	12.30	8.74	1.40	1.25	0,06	2.73
	TEK-03	218.00	13.40	257.00	5.20	24.30	5.50	47.70	40.00	26.00	18.00	4.00	624.00	19.00	76.00	59.90	6.50	17.85	0.90	2.58	0,07	11.52
	LIK-01	244.00	19.70	766.00	11.00	30.40	14.60	58.70	19.00	22.00	44.00	8.00	398.00	12.00	32.00	20.60	18.00	7.32	1.20	1.79	0,14	1.87
	LIK-05	245.00	17.35	628.00	12.20	16.00	11.00	39.90	17.00	28.00	32.00	5.00	476.00	14.00	42.00	15.45	15.00	7.50	0.10	1.42	0,13	1.27
	LIK-07	622.00	3.59	106.00	12.30	22.70	5.30	32.30	74.00	82.00	23.00	13.00	677.00	42.00	60.00	24.50	2.58	9.95	0.40	0.29	0,03	1.99
Lower landsurface relics	TEK-05-a	27.00	10.10	194.00	3.20	4.90	4.70	9.40	18.00	6.00	3.00	2.00	27.00	4.00	20.00	51.90	6.57	14.35	0.20	3.16	0,11	16.22
	LIK-8-a	562.00	16.55	340.00	16.80	8.60	6.30	59.30	22.00	41.00	13.00	1.00	465.00	20.00	29.00	28.20	10.35	6.10	0.00	0.99	0,07	1.68
Lower landsurface granite	R-LO	40.00	14.80	332.00	24.40	1485.00	124.00	2650.00	76.00	15.00	13.00	10.00	80.00	7.00	30.00	19.25	8.50	3.08	0.90	0.61	0.06	0.79

Drc. Rare earth elements

Regolith type	Code	La	Ce	Pr	Nd	Sm	Eu	Gd	Tb	Dy	Ho	Er	Tm	Yb	Lu	Ce/Ce*	Eu/Eu*	(Gd/Yb)N
Upper landsurface ferricretes	SL-2	30.30	58.50	6.23	22.50	3.85	0.84	2.41	0.36	1.85	0.30	0.83	0.13	0.86	0.12	1.00	1.20	1.40
	SL-3	27.60	63.50	5.70	20.90	3.69	0.76	2.34	0.35	1.83	0.32	0.89	0.13	0.88	0.14	1.19	1.12	1.33
	SL-4	23.90	94.30	5.20	19.60	3.64	0.88	2.39	0.38	2.15	0.36	1.06	0.15	1.10	0.17	1.99	1.29	1.19
	SL-5	33.00	60.60	6.18	21.80	3.79	0.82	2.51	0.34	1.97	0.33	0.83	0.12	0.82	0.14	1.00	1.15	1.53
	BIR-01	32.00	59.50	6.13	21.00	3.24	0.57	2.31	0.33	1.76	0.28	0.89	0.10	0.92	0.11	1.00	0.90	1.36
	BIR-02	25.80	49.30	5.15	17.90	2.78	0.48	1.89	0.27	1.46	0.25	0.79	0.09	0.91	0.11	1.01	0.91	1.04
	M-11	34.30	82.80	6.74	22.60	4.19	0.83	2.75	0.37	1.92	0.34	1.07	0.15	0.95	0.12	1.28	1.06	1.45
	MAN-10-1	22.50	42.80	5.17	17.80	3.40	0.58	2.21	0.35	2.05	0.40	1.28	0.18	1.32	0.21	0.93	0.92	0.84
Upper landsurface relics	SL-A	145.50	136.50	21.70	57.40	7.92	1.82	3.73	0.44	1.70	0.23	0.43	0.05	0.29	0.04	0.57	1.45	6.43
	SL-B	49.00	106.00	13.50	54.80	11.35	2.76	7.06	0.86	3.48	0.46	1.05	0.15	0.97	0.14	0.97	1.34	3.64
	SL-C	13.10	19.50	2.59	9.50	1.97	0.47	1.53	0.24	1.25	0.25	0.70	0.11	0.84	0.12	0.79	1.17	0.91
	SL-D	26.20	49.40	5.68	20.70	3.22	0.68	1.97	0.23	0.96	0.16	0.45	0.06	0.40	0.06	0.95	1.17	2.56
	SL-E	64.30	137.50	17.70	74.30	15.70	4.11	11.80	1.42	5.97	0.72	1.44	0.18	1.12	0.16	0.96	1.31	5.37
	BIR-A	16.40	35.80	3.28	11.50	1.96	0.43	1.43	0.19	1.16	0.19	0.65	0.05	0.71	0.08	1.15	1.11	1.01
	BIR-C	16.00	21.80	2.65	8.60	1.41	0.32	1.04	0.14	0.79	0.11	0.44	0.03	0.46	0.04	0.79	1.15	1.13
	BIR-E	145.50	325.00	33.80	118.00	18.25	3.31	11.95	1.53	7.66	1.26	3.16	0.37	2.34	0.25	1.09	0.97	2.65
Upper landsurface granite	R-BIR-02	72.60	151.00	21.30	84.30	15.30	2.62	11.95	1.61	8.97	1.66	4.82	0.63	4.24	0.59	0.90	0.84	1.41
Midlle landsurface ferricretes	KAL-1	23.80	35.30	3.81	11.60	1.84	0.40	1.12	0.18	1.14	0.20	0.62	0.09	0.64	0.11	0.87	1.21	0.88
	KAL-2	23.90	35.00	4.05	13.20	2.04	0.43	1.40	0.21	1.15	0.23	0.62	0.10	0.76	0.11	0.84	1.10	0.92
	KAL-3	19.50	32.30	3.20	10.50	1.62	0.36	1.05	0.17	1.07	0.21	0.63	0.09	0.62	0.10	0.96	1.20	0.85
	KAL-4	22.40	35.10	3.80	12.80	2.09	0.41	1.26	0.21	1.25	0.21	0.62	0.09	0.66	0.11	0.90	1.10	0.95
	KAL-5	21.10	30.50	3.61	11.70	1.89	0.39	1.25	0.18	0.91	0.19	0.55	0.08	0.67	0.10	0.82	1.10	0.93
	LO-1	27.90	65.30	6.10	22.10	3.63	0.72	2.74	0.41	2.41	0.49	1.46	0.22	1.58	0.26	1.18	0.99	0.87
	KAL-01	30.20	48.10	5.08	15.80	2.48	0.49	1.48	0.19	0.92	0.19	0.59	0.10	0.62	0.11	0.91	1.11	1.19
	LIK-08-1	14.50	33.40	3.29	11.60	2.55	0.48	2.41	0.44	3.03	0.64	1.86	0.26	1.96	0.33	1.14	0.84	0.61
	MAN-02	55.50	102.50	11.90	41.40	6.67	1.34	4.28	0.55	2.80	0.48	1.31	0.15	1.11	0.17	0.94	1.09	1.93
	MAN-04	26.90	51.40	5.00	17.00	2.83	0.54	1.83	0.28	1.42	0.27	0.69	0.08	0.84	0.12	1.04	1.03	1.09
Midlle landsurface relics	MAN-03-a	29.60	61.00	6.08	21.30	3.41	0.70	2.19	0.30	1.54	0.28	0.76	0.08	0.64	0.09	1.07	1.11	1.71
	KAL-A	29.40	56.00	4.49	14.20	2.21	0.46	1.54	0.21	1.03	0.22	0.60	0.08	0.65	0.09	1.15	1.08	1.18
	KAL-C	21.40	30.30	3.95	13.20	2.26	0.50	1.57	0.22	1.02	0.22	0.58	0.07	0.57	0.08	0.78	1.15	1.38
	KAL-D	29.60	57.30	5.82	20.30	3.44	0.72	2.41	0.32	1.57	0.31	0.80	0.11	0.69	0.10	1.03	1.08	1.75

	KAL-E	26.30	35.90	4.60	14.30	2.32	0.47	1.56	0.21	1.04	0.19	0.50	0.07	0.52	0.07	0.77	1.07	1.50
	LO-B	67.10	138.00	16.20	61.40	9.44	1.94	5.82	0.66	2.89	0.46	1.19	0.15	1.10	0.15	0.99	1.13	2.65
	KAL-I	16.20	24.70	2.52	8.40	1.48	0.38	1.02	0.12	0.83	0.13	0.36	0.06	0.33	0.06	0.91	1.34	1.55
	KAL-J	35.20	48.20	5.14	14.80	2.08	0.41	1.34	0.19	0.95	0.16	0.45	0.06	0.40	0.07	0.84	1.06	1.68
Middle landsurface granite	R-KAL	62.60	108.00	12.45	42.60	7.18	1.91	5.90	0.73	4.24	0.68	1.75	0.19	1.31	0.17	0.91	1.27	2.25
Lower landsurface ferricrete	HG-01	29.60	61.00	6.08	21.30	3.41	0.70	2.19	0.30	1.54	0.28	0.76	0.08	0.64	0.09	5.08	1.03	0.51
	DIR-01	29.40	56.00	4.49	14.20	2.21	0.46	1.54	0.21	1.03	0.22	0.60	0.08	0.65	0.09	1.15	0.78	0.55
	TEK-03	21.40	30.30	3.95	13.20	2.26	0.50	1.57	0.22	1.02	0.22	0.58	0.07	0.57	0.08	0.80	1.07	1.55
	LIK-01	29.60	57.30	5.82	20.30	3.44	0.72	2.41	0.32	1.57	0.31	0.80	0.11	0.69	0.10	1.16	0.83	0.65
	LIK-05	26.30	35.90	4.60	14.30	2.32	0.47	1.56	0.21	1.04	0.19	0.50	0.07	0.52	0.07	0.91	1.10	0.69
	LIK-07	67.10	138.00	16.20	61.40	9.44	1.94	5.82	0.66	2.89	0.46	1.19	0.15	1.10	0.15	0.57	1.25	1.11
Lower landsurface relics	TEK-05-a	22.00	40.50	3.64	11.20	1.80	0.24	1.14	0.17	0.75	0.13	0.37	0.04	0.55	0.12	1.07	0.73	1.04
	LIK-8-a	12.50	27.00	2.93	10.90	2.17	0.54	2.14	0.42	2.78	0.65	1.98	0.26	1.98	0.31	1.05	1.09	0.54
Lower landsurface granite	R-LO	111.50	222.00	24.90	94.60	15.05	3.01	9.44	1.02	4.98	0.79	2.19	0.26	1.86	0.25	0.99	1.09	2.54